WADC TECHNICAL REPORT 54-615

DETERMINATION OF RESIDUAL STRESSES BY INDENTATION METHODS

R. A. BAREISS

LESSELLS AND ASSOCIATES, INC.

DECEMBER 1954

AERONAUTICAL RESEARCH LABORATORY
CONTRACT No. AF 33(616)-253
PROJECT No. 7351

WRIGHT AIR DEVELOPMENT CENTER
AIR RESEARCH AND DEVELOPMENT COMMAND
UNITED STATES AIR FORCE
WRIGHT-PATTERSON AIR FORCE BASE, OHIO

Carpenter Litho & Prtg. Co., Springfield, O.
200 - 13 July 1955

FOREWORD

This report was prepared by Robert A. Bareiss of Lessells and Associates, Inc., on Air Force Contract No. AF33(616)-253 under Project 7351, Task 70645, "Determination of Residual Stresses." The contract was administered under the direction of the Aeronautical Research Laboratory, Wright Air Development Center, with Mr. James W. Poynter acting as project engineer.

The assistance of the Charles T. Morgan Company during the phases of this test program related to ultrasonic sound waves is gratefully acknowledged.

ABSTRACT

Experimental and mathematical analyses of three promising methods of measuring residual stresses are described. Particular emphasis is placed upon the heavy indentation technique and it is shown how this test can be used to determine the direction and magnitude of uniaxial residual surface stresses. The light indentation technique is also discussed, including a brief study of the possibility of using ultrasonic surface waves as a means of detecting the initiation of plastic flow in the indentation. A mathematical analysis of the drilling out technique is presented directed towards a better understanding of the mechanisms of stress relief using this method.

PUBLICATION REVIEW

This report has been reviewed and is approved.

FOR THE COMMANDER:

Leslie B. Williams

LESLIE B. WILLIAMS
Colonel, USAF
Chief, Aeronautical Research Laboratory

TABLE OF CONTENTS

LIST OF ILLUSTRATIONS

I. INTRODUCTION

A. Background

In recent years the general subject of residual stresses has received an increasing amount of attention from engineers and scientists. It has been demonstrated that unfavorable residual stresses are in many cases the cause of premature failures in machine parts whereas favorable stresses generally prolong the service life, especially where the ultimate failure is due to fatigue. If, then, it is possible to increase the endurance limit of a given part through the proper use of residual stresses, the result will be either a longer life for a given load or a greater load-carrying ability for a given life. This may be an economic gain in that inexpensive materials will be able to serve where previously only high-grade materials sufficed. A further gain would be in the case where a particular requirement exceeded the properties of presently known materials. If it were possible to upgrade a known material to the desired strength or strength-weight ratio by residual stressing techniques, then a benefit of inestimable value would result. The attainment of higher strength-weight ratios is of vital importance to aircraft and missile designers.

The study of this subject may be divided into three logical subdivisions: (1) determination of the effect on service life of stress magnitude and direction, (2) methods of producing favorable stresses and (3) methods of measuring the stresses. Each of these categories has received its share of attention in the laboratories such that the designer may now in some cases specify residual stressing treatments to obtain a desired service life. There remains, however, one break in this growing chain of knowledge which prevents us from taking full advantage of our understanding of the subject. This link which remains to be forged is a nondestructive method for measuring residual stresses which can be used in the inspection of machine parts.

There are a number of methods currently being employed for the determination of residual stresses in metals. Most of these methods are destructive in nature, while the few that are not are restricted to particular types of materials and are semiquantitative only. The destructive, or relaxation methods, rely upon the removal of the residual stresses in controlled increments by removing some of the stressed material. The stresses in the portion removed are then determined as a function of the change in shape or strain in the piece remaining. This method was first suggested for cylindrical parts and has since been extended to more general cases. This technique has been enhanced in recent years by the development of electro and acid-etch procedures for removing material.

Drilling out is another of the relaxation methods wherein only a relatively small plug of material is removed rather than entire surface layers. The principle, however, is quite similar.

The nondestructive techniques currently employed are somewhat more indirect in that they measure some condition of the material other than stress or strain but which may be correlated with residual stress. For example, in the case of X-ray techniques distortions in the atomic lattice spacing are determined, while in the case of magnetic methods changes in orientation of magnetic domains are generally the measured parameter. In this latter case the measurement may be either a bulk determination of permeability or an

observation of the magnetic domains themselves through the use of a technique developed by Bitter (1)* and recently extended by Dykstra (2) et al.

In both of the instances mentioned above, the restrictions as to the types of materials which may be tested are quite severe. Radiographs become quite difficult to analyze for materials other than the simple alloys free of plastic strain, while the magnetic methods mentioned are limited to ferromagnetic materials.

It becomes apparent from these few brief considerations that there is a need for a residual stress measuring technique which will satisfy three principle requirements: (1) it must be nondestructive for use in production control, (2) it must be applicable to a wide range of materials, (3) it must have a facility of use in order that it may be readily employed in the field.

B. Scope of Work

In the first technical report written under this contract, WADC TR 54-3, Brodrick described the very broad range of potential new methods which were studied for possible development. Preliminary experimental consideration of some of the more promising concepts were also outlined in some detail. The present report recounts the continued investigation of the two methods which were considered to be most applicable.

The first of these is the ball indentation method which is divided into two categories. The heavy indentation technique carries the process well into the plastic range and requires the measurement of strains on the surface of the test material surrounding the indentation. The light indentation technique requires the detection of the indentor force which causes the first departure from the elastic case.

The drilling out method was the second one to be considered in this work. On the following pages the particular approach to each of these problems is discussed in some detail.

II. HEAVY INDENTATIONS

A. Theoretical Considerations

A theoretical analysis of the actions and reactions due to a spherical indentor penetrating a surface was undertaken in order to determine the significant parameters related to residual stress. Because of the complex nature of this problem resulting from the combined elastic-plastic state of the material under test, this analysis was limited to qualitative considerations.

Consider first the case of indenting a surface which is free of all residual stresses. The results of this indentation are shown schematically in Figure 1.

* Numbers in the parenthesis refer to the Bibliography.

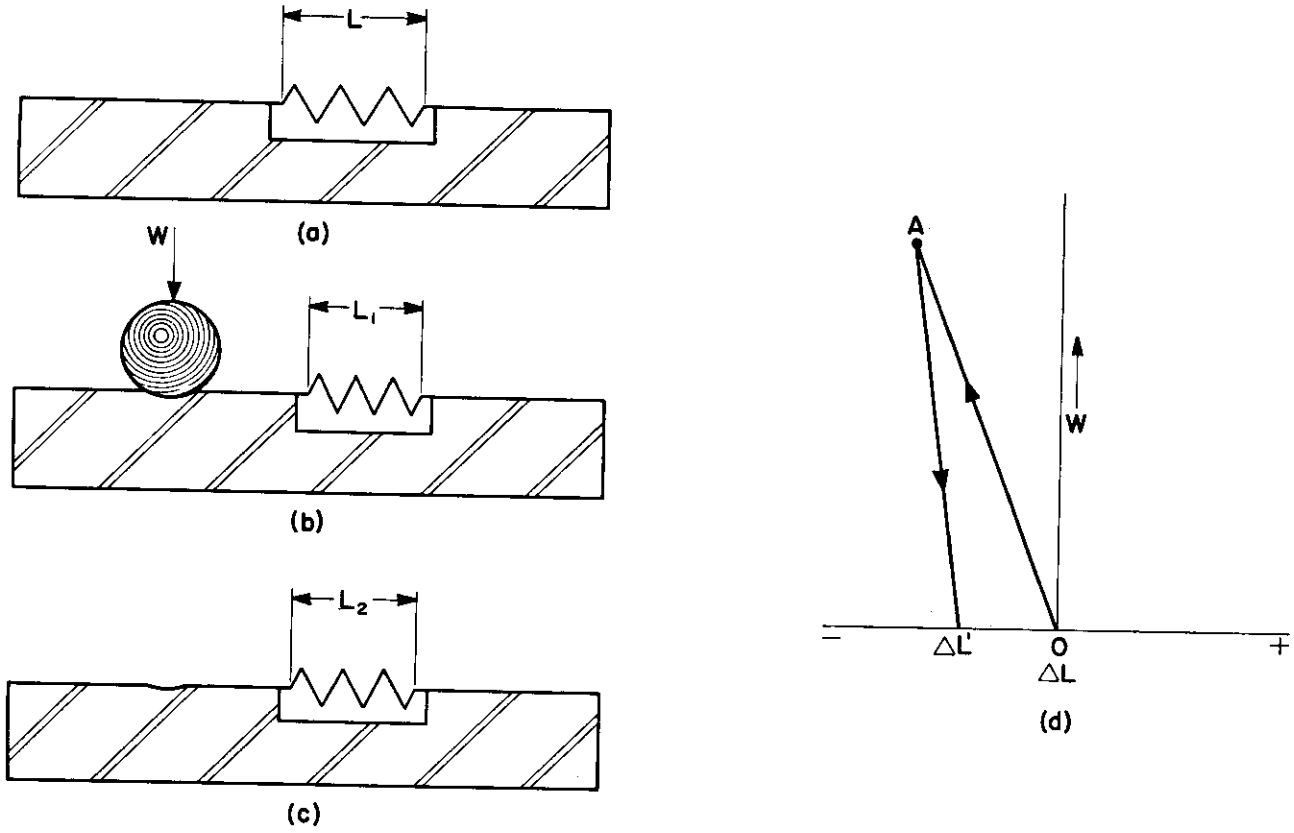

Figure 1. Schematic Representation of the Indentation Process - Stress-Free Surface

In Part (a) of this figure a section of the surface is removed and replaced by an unstressed spring of length L. In (b) a spherical indentor is brought into contact with the surface under the action of a load W. The point of contact of the indentor is located such that the plasticized region in the surface will not extend out to the spring. The surface stresses due to this indentation process are compressive and thus the spring is shortened to some length L_1. In (c) the indentor has been removed, the entire surface returns to the elastic condition and the compressive stresses due to the indentation are relieved to the extent permitted by the new state of the surface. The spring now attains a length L_2 which is between L and L_1 in magnitude. These results are shown graphically in (d) where the change in spring length, ΔL, from its initial length L, is plotted against the indentor load, W. The line O→A represents the indentor loading process while the line A→$\Delta L'$ represents the unloading process. The value $\Delta L'$ is a measure of the residual compressive stress due to the indentation.

Consider next the case of a surface which contains uniaxial tensile residual stress as shown in Figure 2.

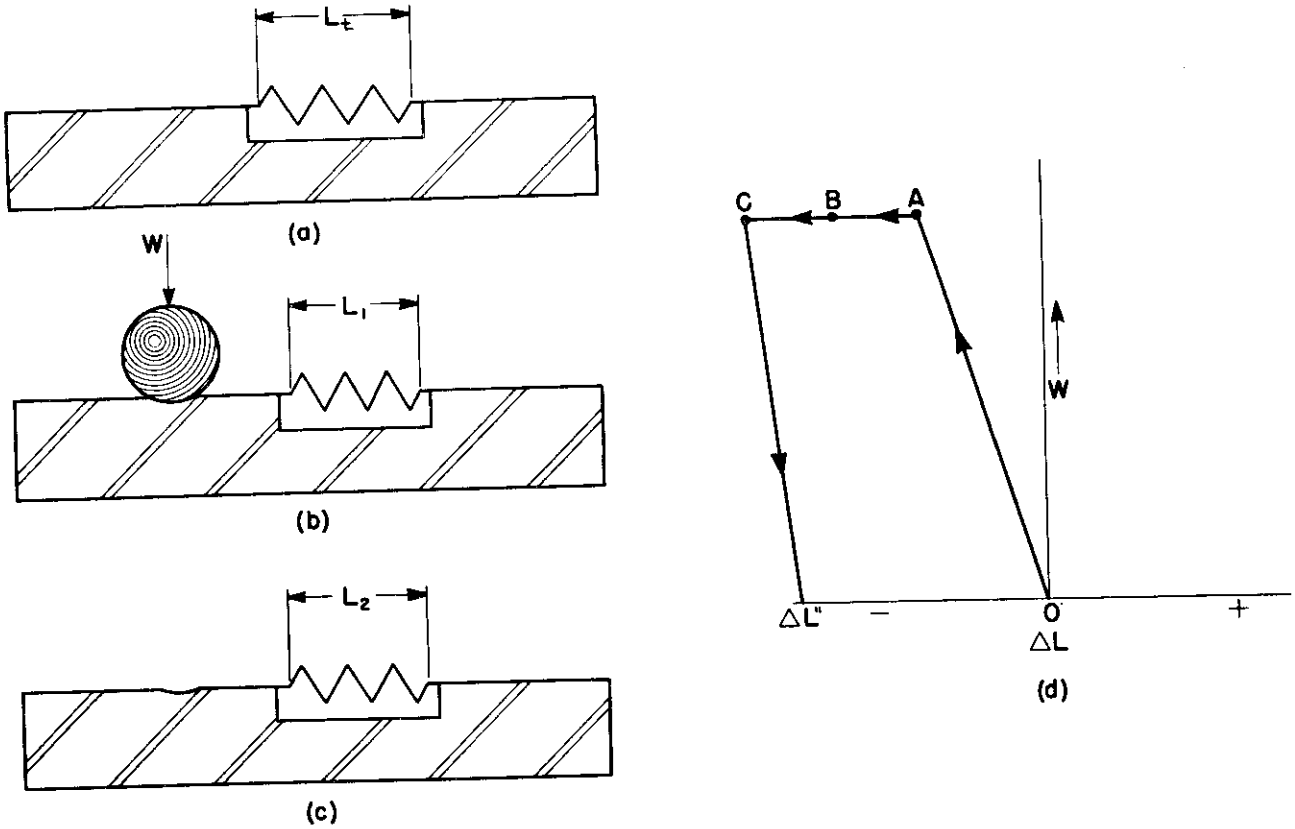

Figure 2. Schematic Representation of the Indentation Process - Tensile Surface Stresses

In(a), as in the previous example, a section of the surface is removed and replaced by a spring which in this case is stressed in tension to some length L. Once again the initial result of applying the indentor to the surface with the load, W, is a compressive stress in the spring as shown by the line O→A in (d). The indentation, however, acts as a stress reliever with respect to the initial stress in the surface resulting in further changes in the spring length. As these initial stresses were tensile their relief results in a shortening of the spring or a compressive value of ΔL, where ΔL is the change in length from the value L_t.

This stress relief is the result of two different aspects of the indentation process. In the first instance the indentation is a discontinuity with respect to the surface, partially removing the restraint which was necessary to develop the tensile stresses initially present. Secondly, the plasticized region which exists in the neighborhood of the indentation while the indentor is in place serves to further reduce the initial restraint. In Figure 2, Part (d), the results of this two-part strain relief are shown as the lines A→B, and B→C. Upon removing the indentor, there is again a partial relief of the elastic compressive stresses due to the indentation along the line C→$\Delta L''$. It is seen that

the difference between the change in spring length in the stress-free case $\Delta L'$ and the tensile case $\Delta L''$ is equal to the residual stress parameter A→C.

$$\Delta L' - \Delta L'' = A \rightarrow C$$

The last case to be considered is that of a residual uniaxial compressive stress in the surface. Once again, as in the previous two examples, the spring analogy is used, Figure 3.

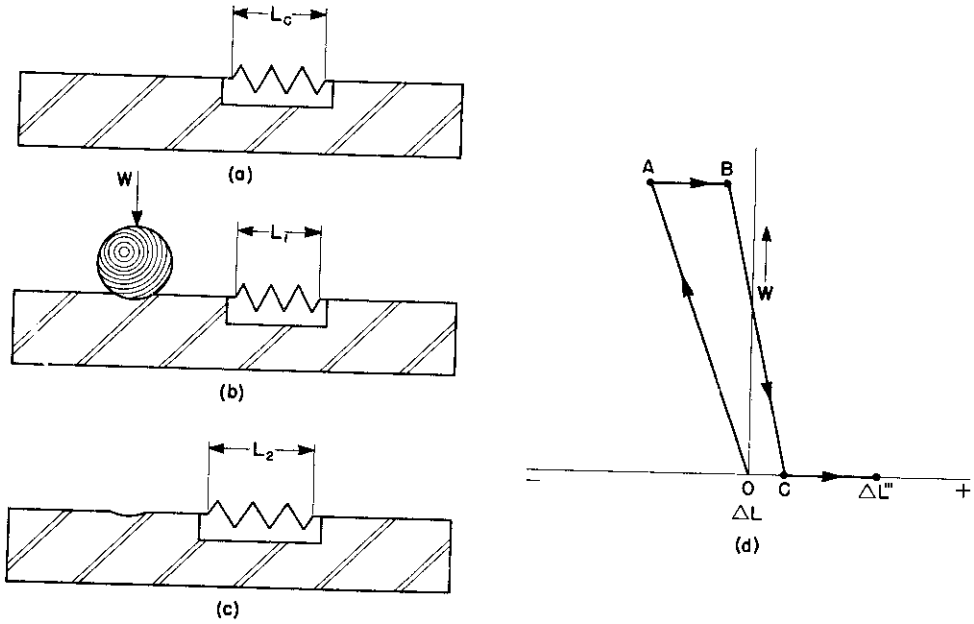

Figure 3. Schematic Representation of the Indentation Process - Compressive Surface Stresses

As before, the initial result of the indentation process is given by the line O→A in (d). Upon reaching the indentor load W the initial compressive stress is partially relieved as in the tensile case but only to the extent permitted by the plasticized region. As this is a relief of compressive stress, the spring elongates giving rise to positive values of ΔL when L is taken as the initial length. This result is indicated by the line A→B.

If residual compressive stresses in a surface are relieved by a discontinuity in the surface, the resultant displacements will be toward the center of the discontinuity. It is readily seen, however, that while the indentor is in contact with the surface and subject to the load W these displacements are effectively blocked and this phase of stress relief cannot take place. Upon unloading, the stresses due to the indentation are partially relieved, as before, along B→C. With the indentor removed, the relief of the initial stress, due to the discontinuity in the surface, now takes place along C→$\Delta L'''$. As in the case of the tensile residual stress, the final value of $\Delta L'''$ is related to the initial residual stress as follows:

$$\Delta L' - \Delta L''' = A \rightarrow B + C \rightarrow \Delta L'''$$

It is realized that this discussion is an oversimplification of the phenomenon, but it at least serves to point out the trend which might be expected in the results of tests conducted to bear out these conclusions. Furthermore, as only the qualitative nature of these reactions has been considered, experimental work is required in order to obtain quantitative results.

B. Test Procedure

1. Introduction

On the basis of results obtained in the theoretical analysis, a series of tests were planned with the purpose of obtaining qualitative data in order to determine the usefulness of the technique. The experimental program was designed to duplicate as nearly as possible the procedure outlined in the theoretical analysis.

2 Test Specimens

Particular attention was given to the design of the test specimens, especially with regard to the manner of introducing residual stresses. Mechanical loading techniques were employed, being the simplest, most direct, and most accurate means of producing controlled stresses of known magnitudes and directions. The stress patterns induced in this manner can be accurately determined through the use of SR-4 wire resistance strain gages bonded to the surface of the test piece. Two different loading techniques were employed. In the first, simple-uniaxial tensile and compressive stresses were induced in the test piece, shown in Figure 4(a), by mounting the specimen in clamping fixtures and loading it between the platens of an horizontal hydraulic testing machine. The uniformity of the longitudinal stress was determined by means of Gages 1, 4, and 5 while the actual stress pattern in the test surface was calculated through the use of data obtained from Gages 1, 2, and 3.

In the second loading technique, test specimens, as seen in Figure 5(a), were loaded in plane bending. The bending moment diagram for this case showing a constant surface stress over the central portion of the test plate is given in Figure 5(b). With this type of loading the stresses vary linearly through the thickness from a maximum on one surface to a maximum of opposite sign on the other surface.

Figures 6(a), (b) and (c) show the three types of loading fixtures used to obtain the stress patterns described above.

In order to get data for materials with different properties, several groups of test specimens were used according to the following tabulation:

GROUP A

Loading - Simple Tension and Compression
Material - 1018 Steel - 1/4 in. Thick
Heat-Treatment - Stress-Relief Anneal
Yield Strength - 35,000 psi
Hardness - R_a35
Surface Finish - Ground

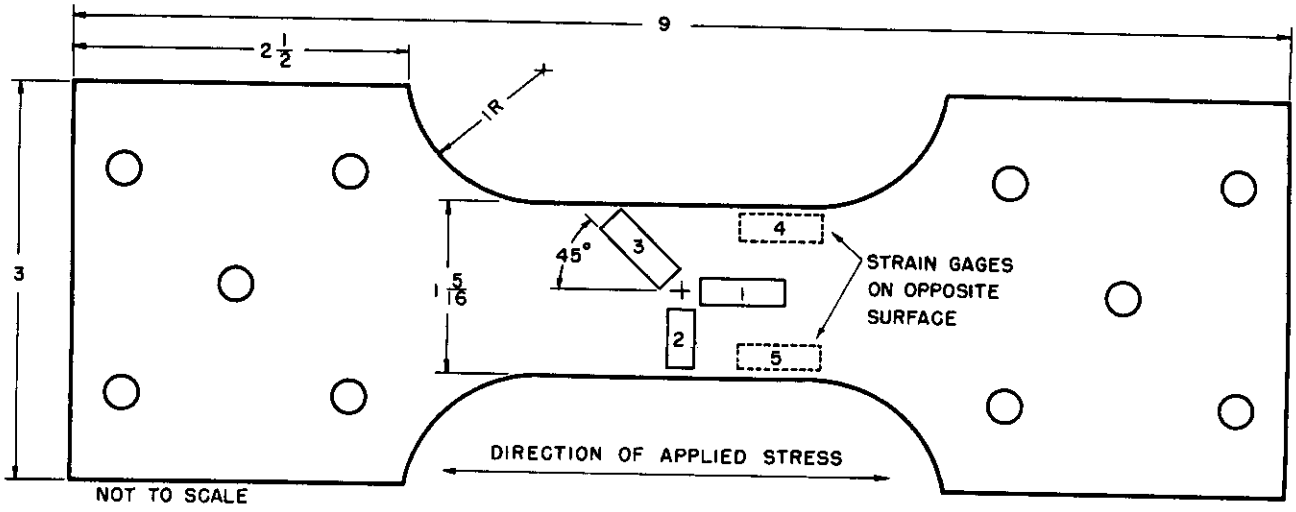

FIG. 4 TEST SPECIMEN FOR SIMPLE TENSION AND COMPRESSION

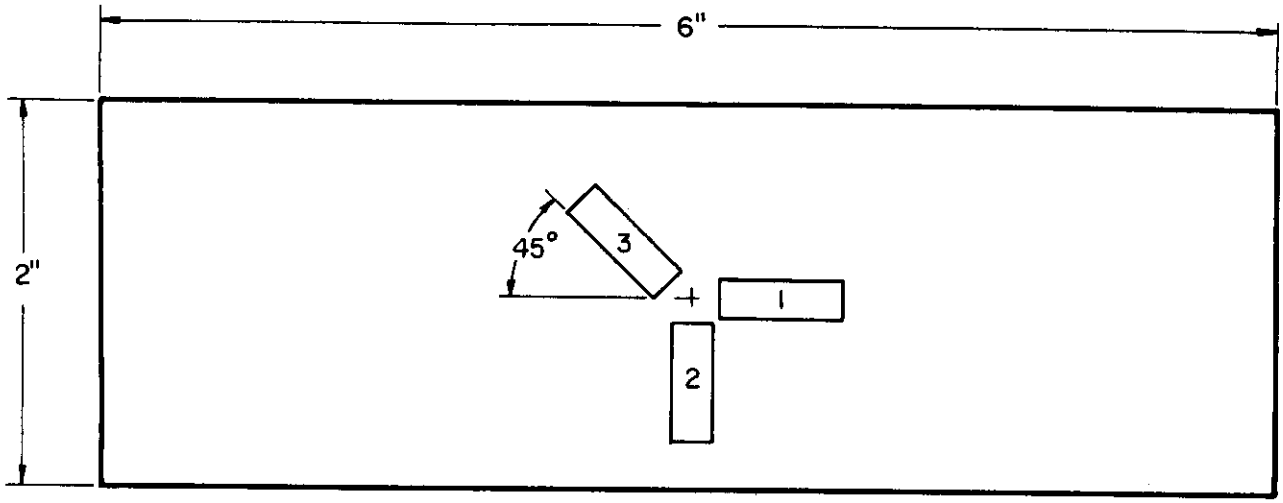

(a)

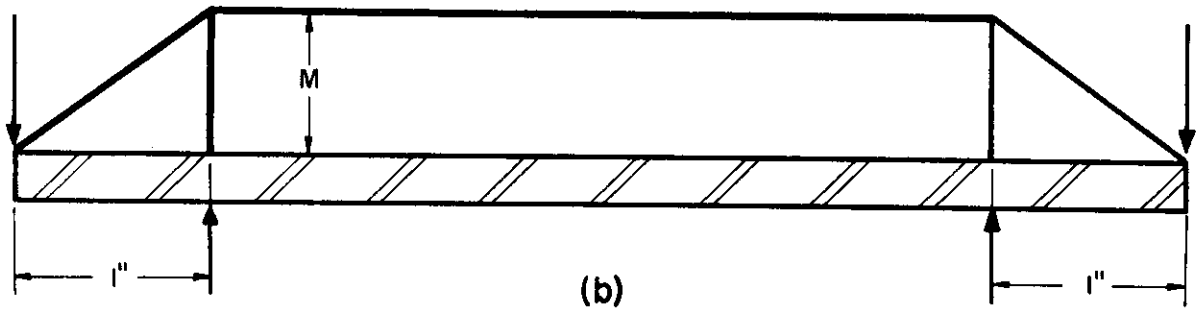

(b)

BENDING MOMENT DIAGRAM

FIG. 5 TEST SPECIMEN FOR PLANE BENDING

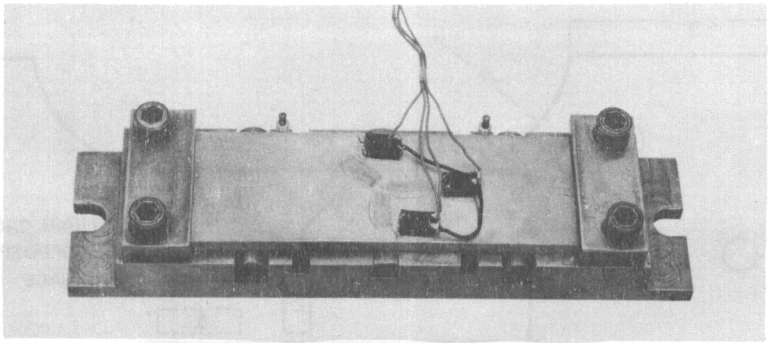

Figure 6(a) Test Fixture - Plane Bending, Tension

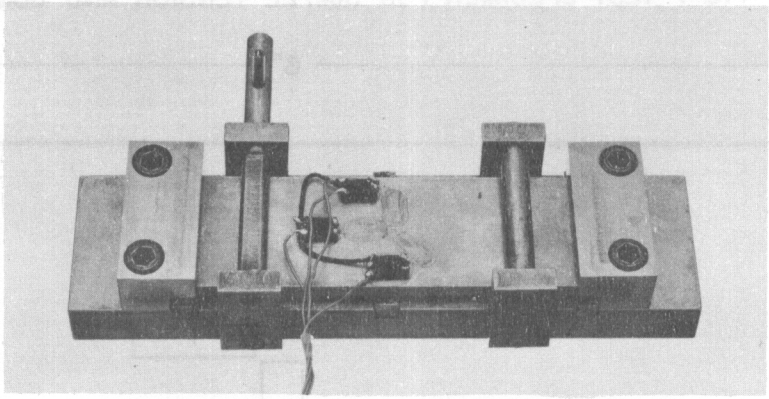

Figure 6(b) Test Fixture - Plane Bending, Compression

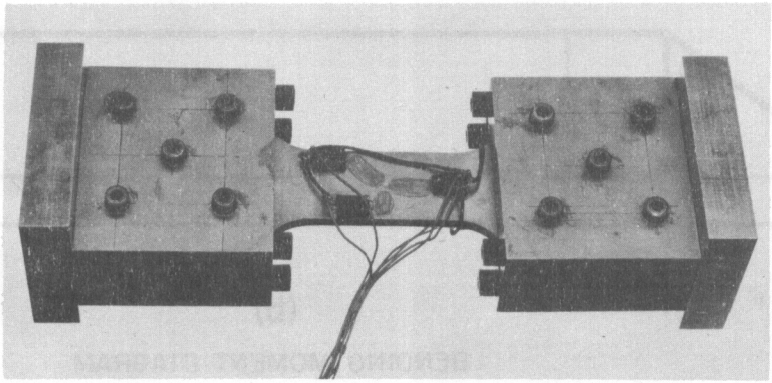

Figure 6(c) Test Fixture - Simple Tension and Compression

GROUP B

Loading - Plane Bending
Material - 1018 Steel - 1/4 in. Thick
Heat-Treatment - Stress-Relief Anneal
Yield Strength - 35,000 psi
Hardness - R_a35
Surface Finish - Ground

GROUP C

Loading - Plane Bending
Material - .90C Alloy Steel - 1/4 in. Thick
Heat-Treatment - Stress-Relief Anneal
Yield Strength - 97,500 psi
Hardness - R_c18
Surface Finish - Ground

3. Indentor

In all of the tests reported here the indentor used was a carbide ball, 10 mm in diameter. The indentor load was applied by an hydraulic piston and measured by a calibrated Bourdon tube-type pressure gage.

4. Surface Strain Measurements

All strain measurements on the surface of the test bars were made through the use of SR-4 wire resistance strain gages. The Type A-7-1 gage was chosen because of its minimum dimensions for the active element area. This was deemed important due to the highly directional properties of the test resulting from the uniaxiality of the applied stresses and further because preliminary tests had indicated that steep strain gradients might be expected in the region of the indentation.

A rectangular rosette pattern was chosen with one gage parallel to the direction of the applied stress as seen in Figures 4 and 5(a). It was necessary to locate the strain gages radially such that they would be outside the region of plasticization surrounding the indentor for all combinations of indentor size, indentor load, and material hardness. A nominal dimension of .125 in. from the center of the indentation to the leading edge of the gage element was determined as an optimum value.

5. Test Method

Approximately seventy individual tests were conducted covering the four specimen groups using the following method.

Each specimen was loaded to a predetermined stress level within the range from approximately 90% of the yield strength in tension to approximately 90% of the yield strength in compression. The indentor was then applied at the center of the strain gage rosette with increasing load increments of 100 lb from 0 to 1400 lb. The indentor was removed after each load increment and the signal from each of the three strain gages was determined both with the indentor loaded and the indentor removed.

Figure 7 shows a test in progress on a specimen stressed in simple compression while Figure 8 is a test in plane bending.

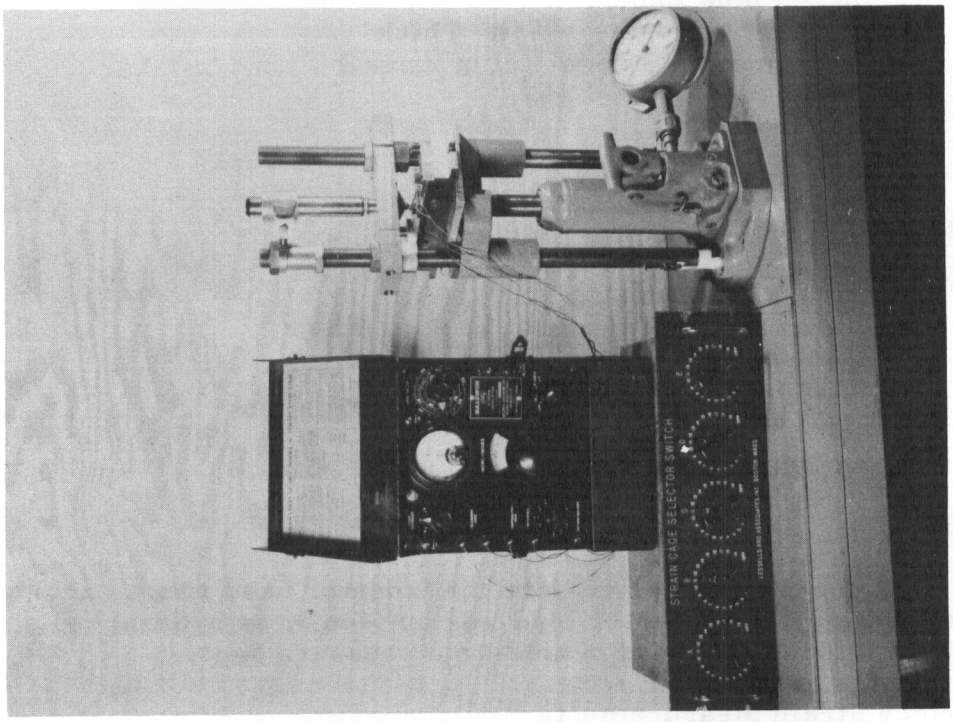

Figure 8. Test in Plane Bending

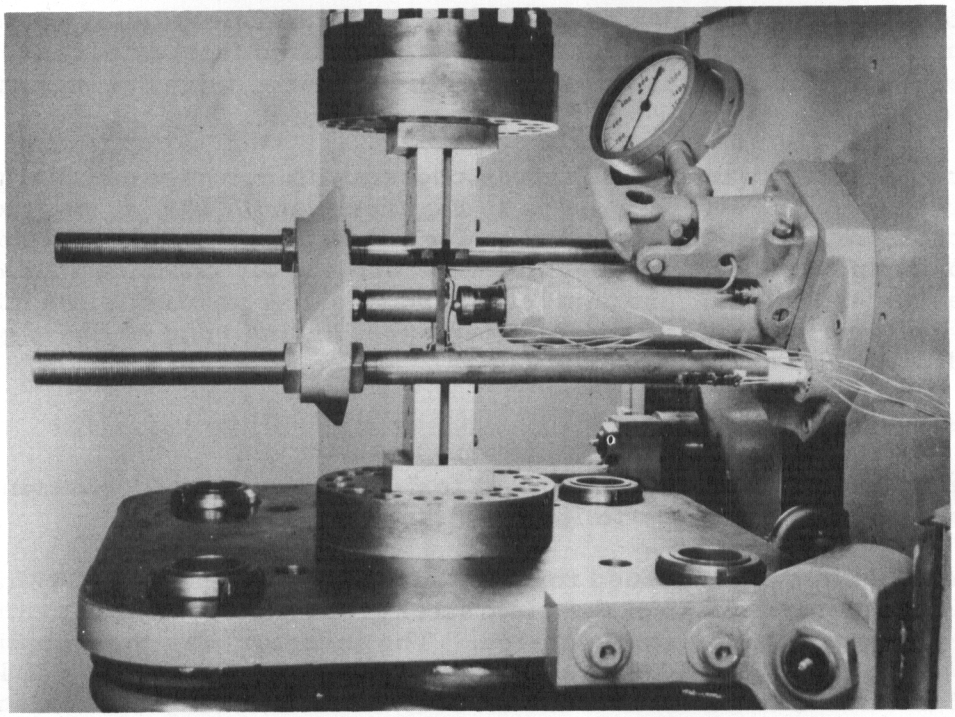

Figure 7. Test in Simple Compression

C. Results.

The data obtained in the experimental phase of this work substantiated conclusively the behavior predicted in the theoretical analysis and supplied the necessary quantitative information to make the test applicable to the determination of residual stresses in machine parts. A great deal of data was obtained during the course of the test program and a step by step analysis is required in order to point out the many ramifications of this technique.

The first tests were carried out on annealed mild steel specimens with no externally applied stresses. The results of these initial tests are presented graphically in Figure 9 where the strains due to indentation have been plotted for the two cases of indentor loaded and indentor removed. The difference between the two strain values at any given load is a measure of the elastic recovery of the indentation upon removing the indentor. The compressive strains which remain after removing the indentor are a result of the residual compressive stresses introduced by the indentation process. These strains are equivalent to $\Delta L'$ in Figure 1.

A number of tests were next conducted on annealed mild steel specimens stressed in simple tension to a nominal value of 30,000 psi. A consideration of the Mohr's circle diagram for this simple loading condition reveals the stresses in each of the three gage directions 1, 2, and 3 are +30,000 psi, 0 psi, and +15,000 psi, respectively. Figure 10 is a representative plot of the strains due to indentation for this test condition. The numbers shown in this and subsequent figures refer to the strain gage locations given in Figures 4 and 5. This data shows quite clearly that the indicated strain due to the indentation is a function of the residual stress pattern in the test piece. In the case of Gages 1 and 3 where the applied stresses are tensile, the indentation strains are more compressive than those obtained for zero stress.

In the direction at right angles to the applied stress, represented by Gage 2, the residual stress is zero, as previously stated, if the load application is strictly uniaxial. However, there are residual compressive strains in this direction related to the strains in the longitudinal direction through Poisson's ratio. The indicated strains at Gage 2 as a result of the indentation are therefore a measure of these compressive strains, being less compressive than those obtained for zero stress. It will be further noted that in the case of Gage 2 the indicated strains with the indentor removed are more compressive than those with the indentor loaded, contrary to the anticipated result. This effect might very well be due to a difference in the distribution of the applied stresses around the indentation with the indentor loaded and the indentor removed.

Of further interest is the fact that the indicated strains for Gages 1 and 3 become only slightly less compressive upon removing the indentor. This bears out the contention that stress relief is completed during the indentation process when the residual stresses are tensile; the slight change in strains when the indentor is removed being a result of elastic recovery of the indentation.

Figure 11 is a representative plot of data obtained from a similar group of tests on specimens externally stressed in simple compression to a value of 30,000 psi As in the previous example, the indicated strains at the maximum value of indentor load are related to the residual strains in the material; i. e., the more compressive the residual strain the less compressive are the indicated strains due to indentation. The data from all three gages in this particular test shows that the stress relief is not complete until the indentor is removed. This is true even for Gage 2 where the residual strains are

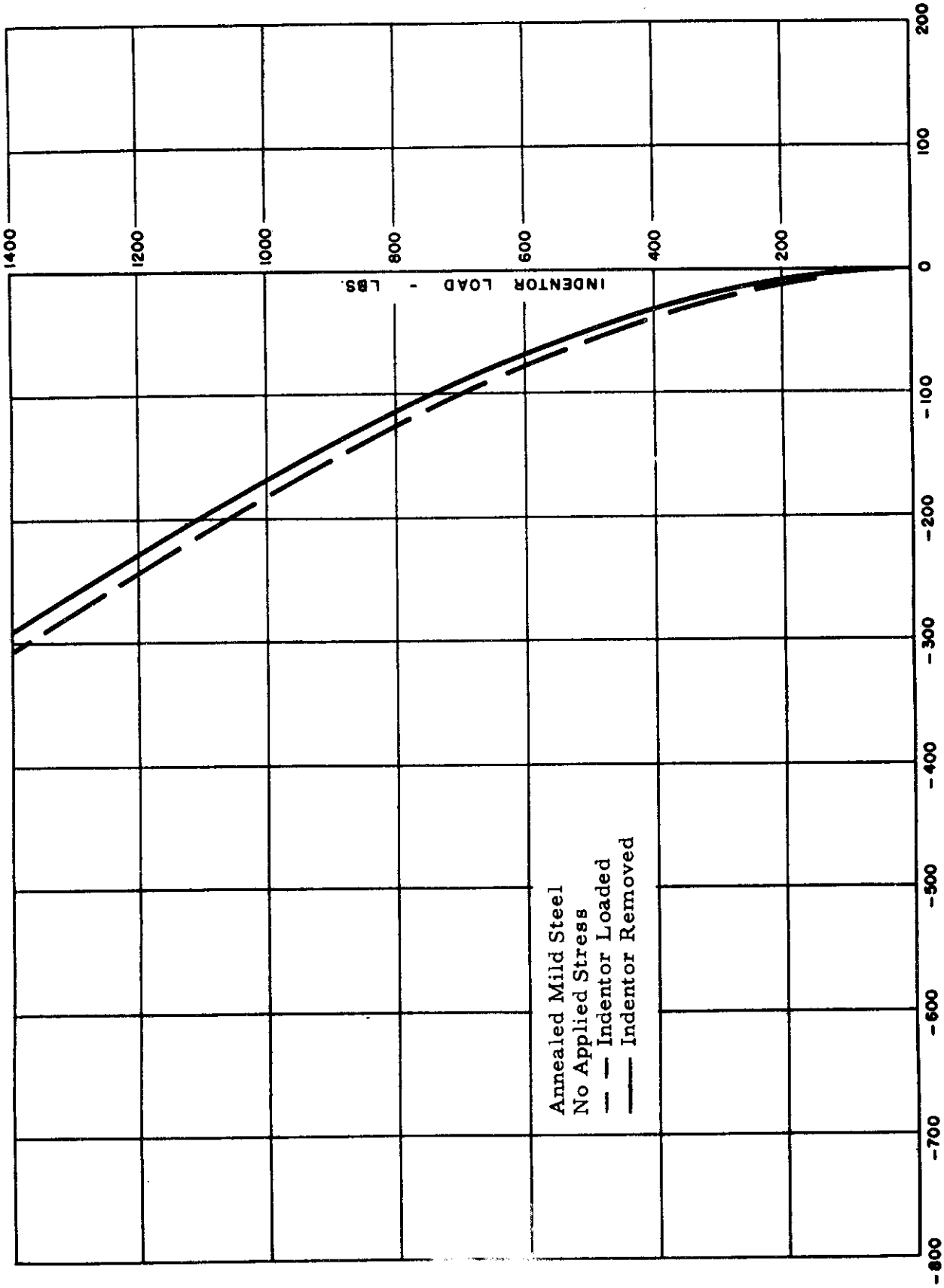

FIG. 9 STRAINS DUE TO INDENTATION

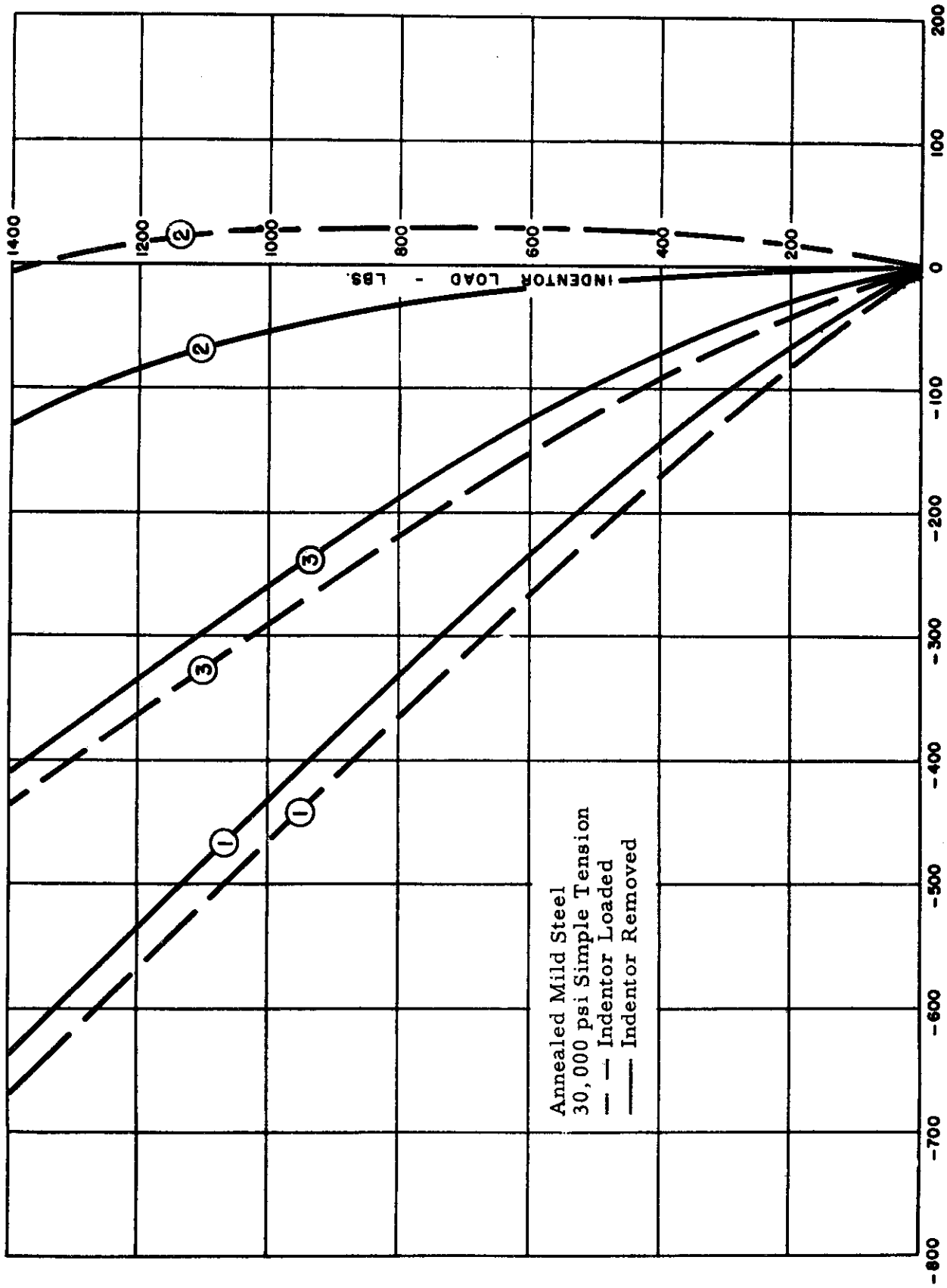

FIG. 10 STRAINS DUE TO INDENTATION

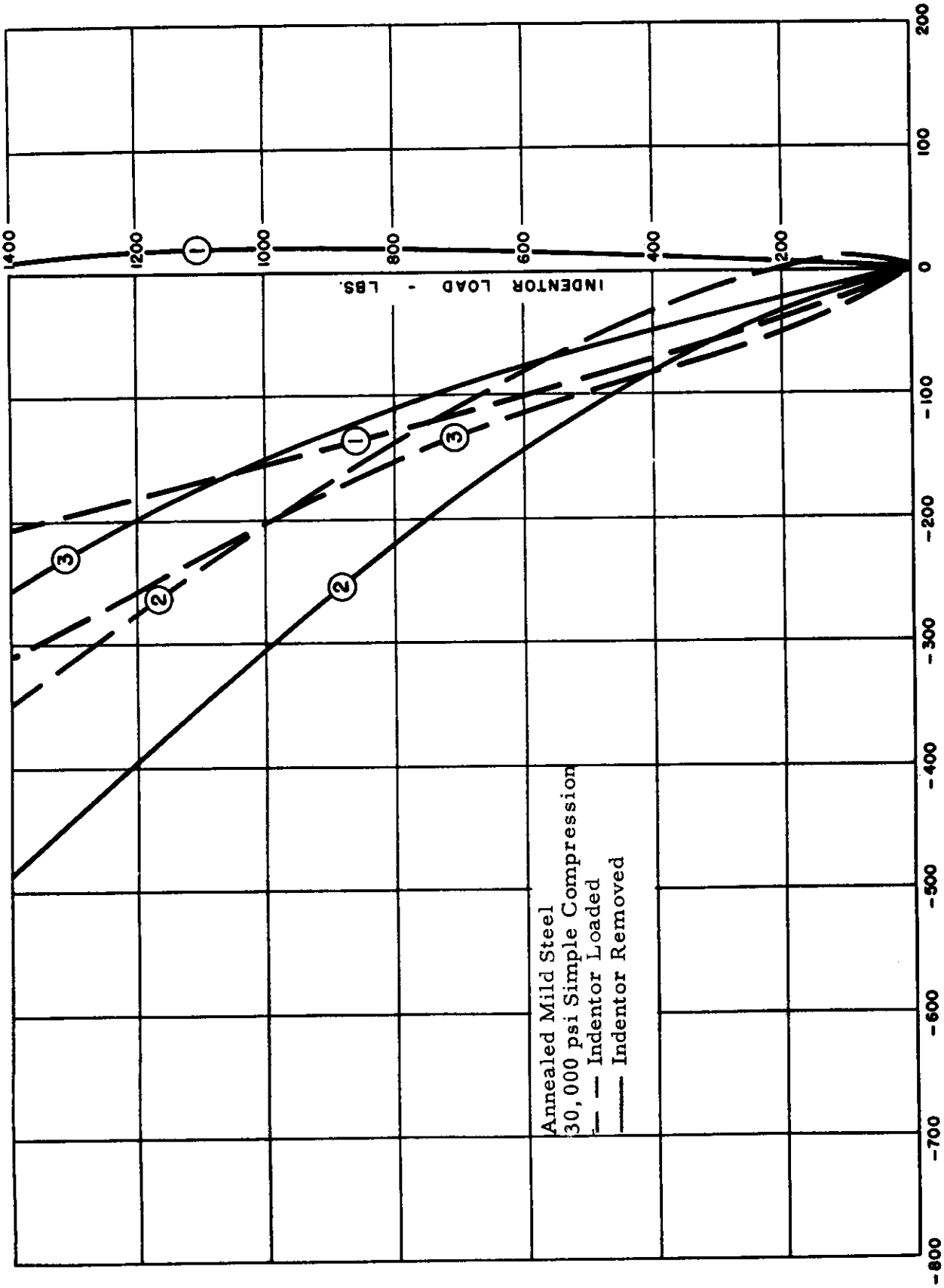

FIG. 11 STRAINS DUE TO INDENTATION

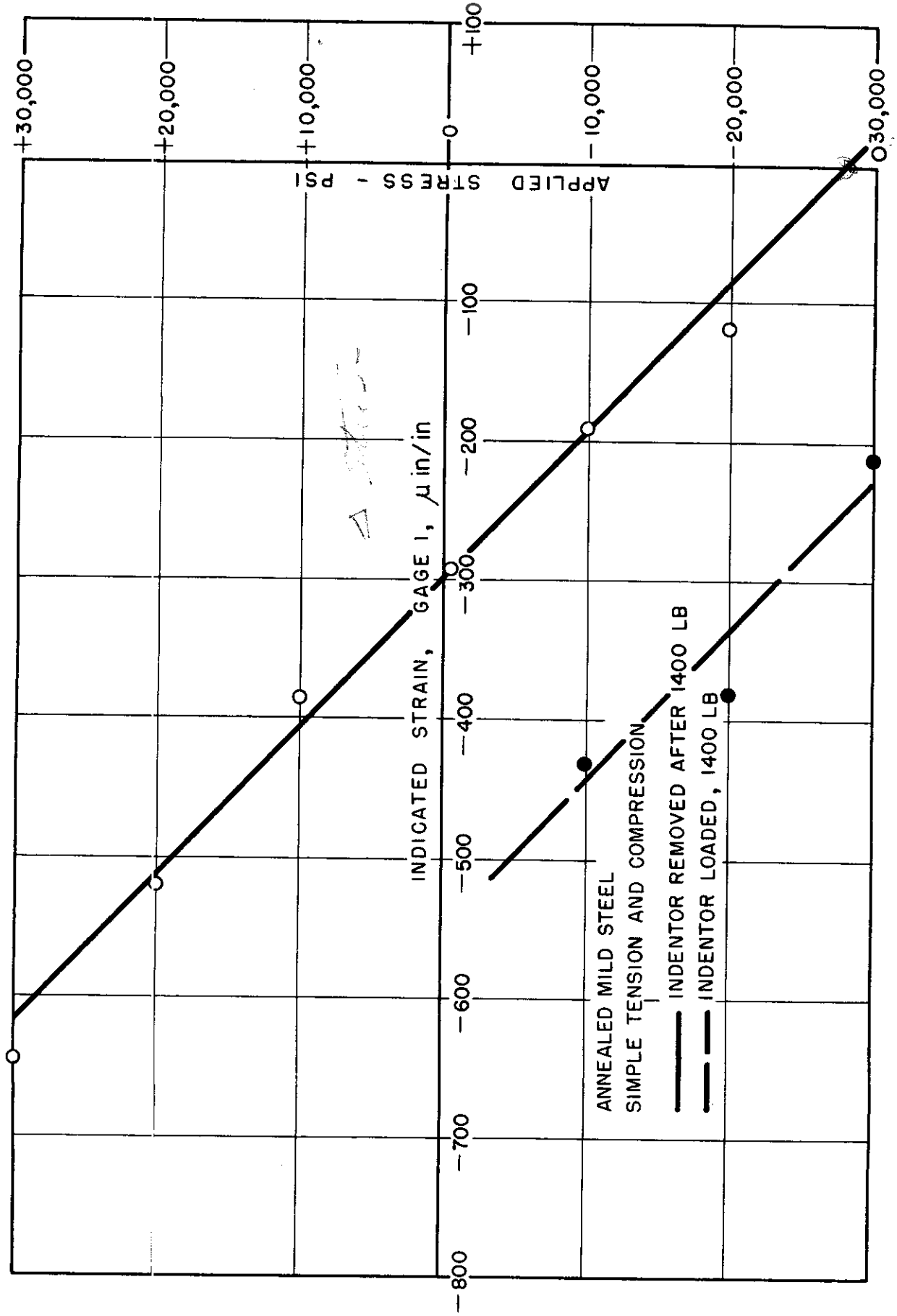

FIG. 12 CORRELATION BETWEEN INDENTATION STRAINS AND RESIDUAL STRESS

tensile because these strains are due to the compressive stress in the longitudinal direction and are, therefore, relieved only to the extent that the longitudinal stresses are relieved.

This same pattern of results holds true for the other values of externally applied stress at which tests were conducted. These results are shown graphically in Figure 12 where the indicated strain values for Gage 1 have been plotted against the applied stress in the test specimen. The linear relationship between applied stress and the indicated surface strains after the indentation is quite apparent. The data for the indentor loaded has also been presented in this figure where the applied stresses are compressive, in order to point up again the two phases of stress relief, one due to the plasticized region and the other due to the discontinuity in the surface.

Several tests were conducted at an applied stress of 30,000 psi in tension with slight variations in the radial location of Gage 1 in order to obtain some information with regard to the radial strain gradient surrounding the indentation. The results of these tests are presented in Figure 13. The scatter in these results is attributed to variations in the residual stresses in the test pieces prior to testing. Stress measurements using relaxation techniques were made on several of the test specimens indicating that residual stresses of varying magnitude were present in a very shallow surface layer in spite of the stress-relief anneal which these specimens were given.

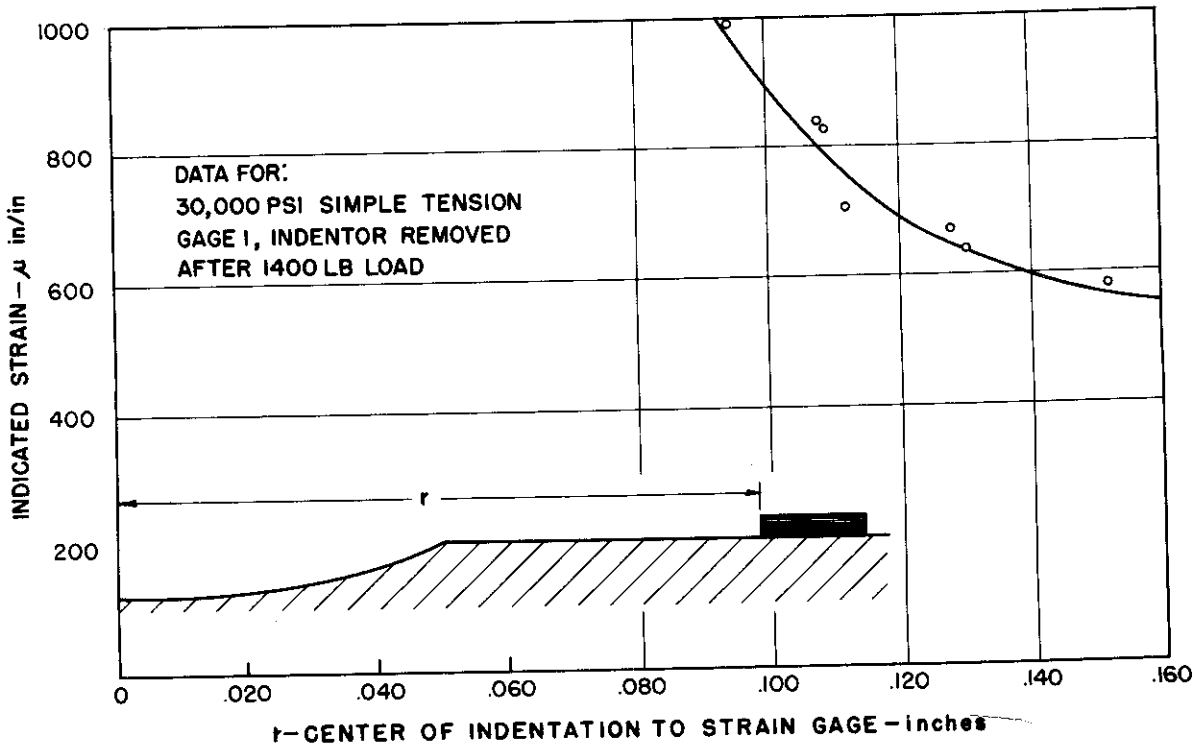

Figure 13. Indentation Strain as a Function of Radial Location

A series of tests similar to those described above were conducted on mild steel test specimens which were loaded in plane bending as described under Test Procedure. The primary purpose of these tests was to determine the feasibility of this much simpler loading technique when compared to simple tension and compression. The results of these tests are shown in Figure 14, a plot similar to Figure 12, and it may be readily seen that the agreement is quite good. For these reasons this method of loading was used for subsequent tests.

The next set of tests was conducted on annealed 0.90 carbon alloy steel plates externally stressed in plane bending. As the yield strength of this material is much higher than that of mild steel, tests at much higher stress levels could be carried out. The maximum stress used was 90,000 psi or 3 times that possible with the mild steel plates. The results of these tests were quite similar qualitatively to the work described above and they are presented here in detail to point out the quantitative variances.

Figure 15 is a plot of the indentation strains without applied stress. In comparing these curves with Figure 9, the data for the mild steel specimen, it is seen that the change in strain upon removing the indentor is considerably more pronounced for the alloy steel, indicating a much greater elastic recovery of the indentation strains.

Figures 16 through 21 are plots of the indentation strains at various values of applied stress for the alloy steel test specimens. The statements which were previously made describing the data for the tests on mild steel hold true for this case and need not be reiterated in detail here.

The indicated strain upon removing the indentor is a linear function of the applied stress in the case of Gage 1, as shown in Figure 22. The data for mild steel is also shown on this plot for purposes of comparison. The differences in slope and position along the strain axis for these two data plots may be attributed directly to the differences in hardness and yield strength of the two materials. These indicated strain values are a function of the stress relief at any particular stress level and will therefore be affected by the amount of stress relief which takes place. The strength and hardness of the material being tested will have a bearing on both phases of the stress relief which have been described above. The basic strength will determine the extent of yielding around the indentation and therefore the degree of relief due to plasticization. The hardness will determine the size of the indentation for any given indentor load and therefore the degree of relief due to surface discontinuity. The alloy steel, being both stronger and harder than the mild steel, will show less stress relief for a given indentor size and load than the mild steel. The indentation diameters, after applying a 10 mm ball with a 1400 lb load, were .100 in. and .085 in. respectively for the mild steel and alloy steel. Furthermore, the residual compressive stresses due to the indentation process itself will be less for the alloy steel as demonstrated by the strain data with no applied stress. This is another effect of the higher yield strength of this material. The net result of these factors, as seen in Figure 22, is a shift in the data for alloy steel toward less compressive strains on the zero stress line and a steeper negative slope as a result of the reduced stress relief for both tensile and compressive applied stresses.

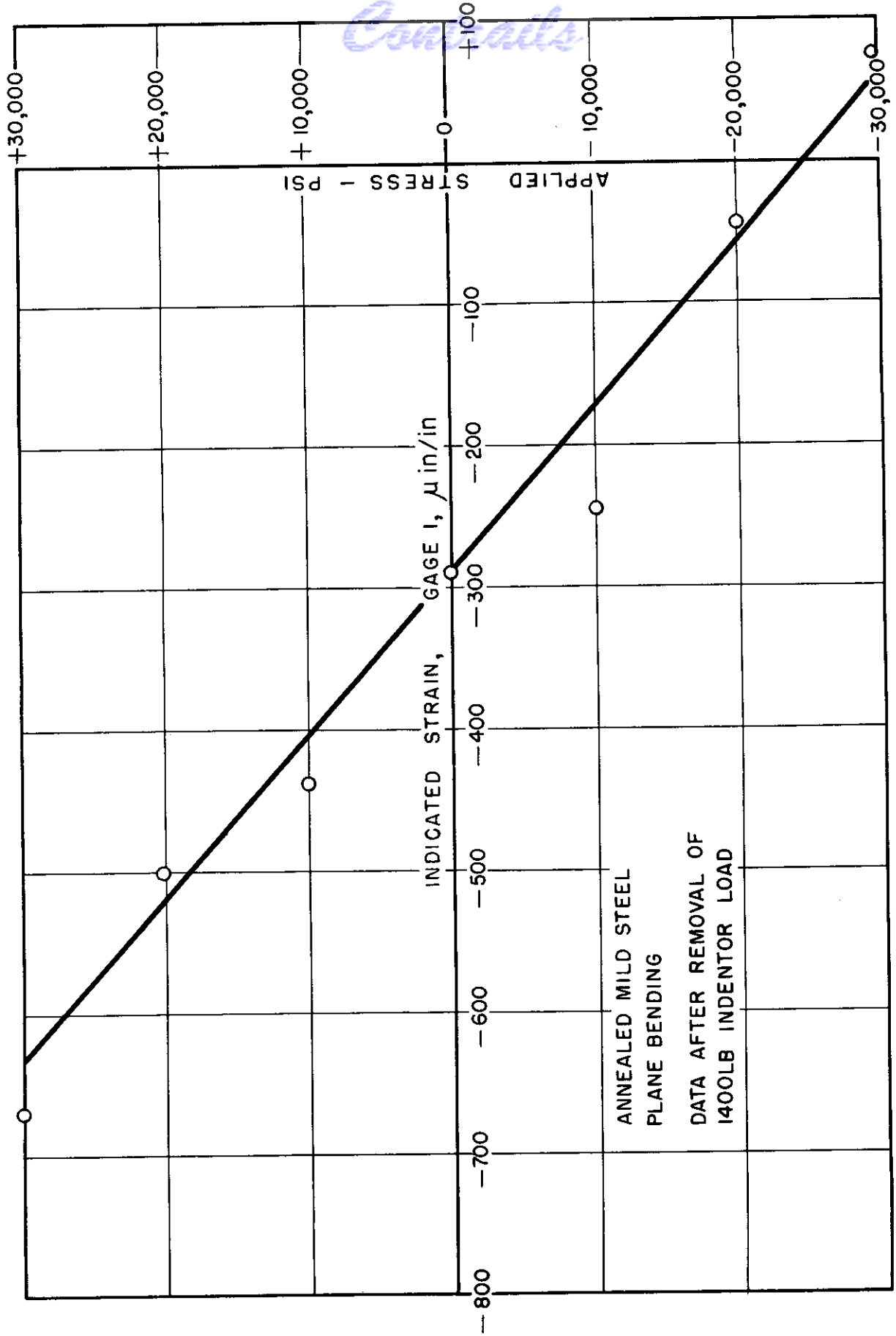

FIG. 14 CORRELATION BETWEEN INDENTATION STRAINS AND RESIDUAL STRESS

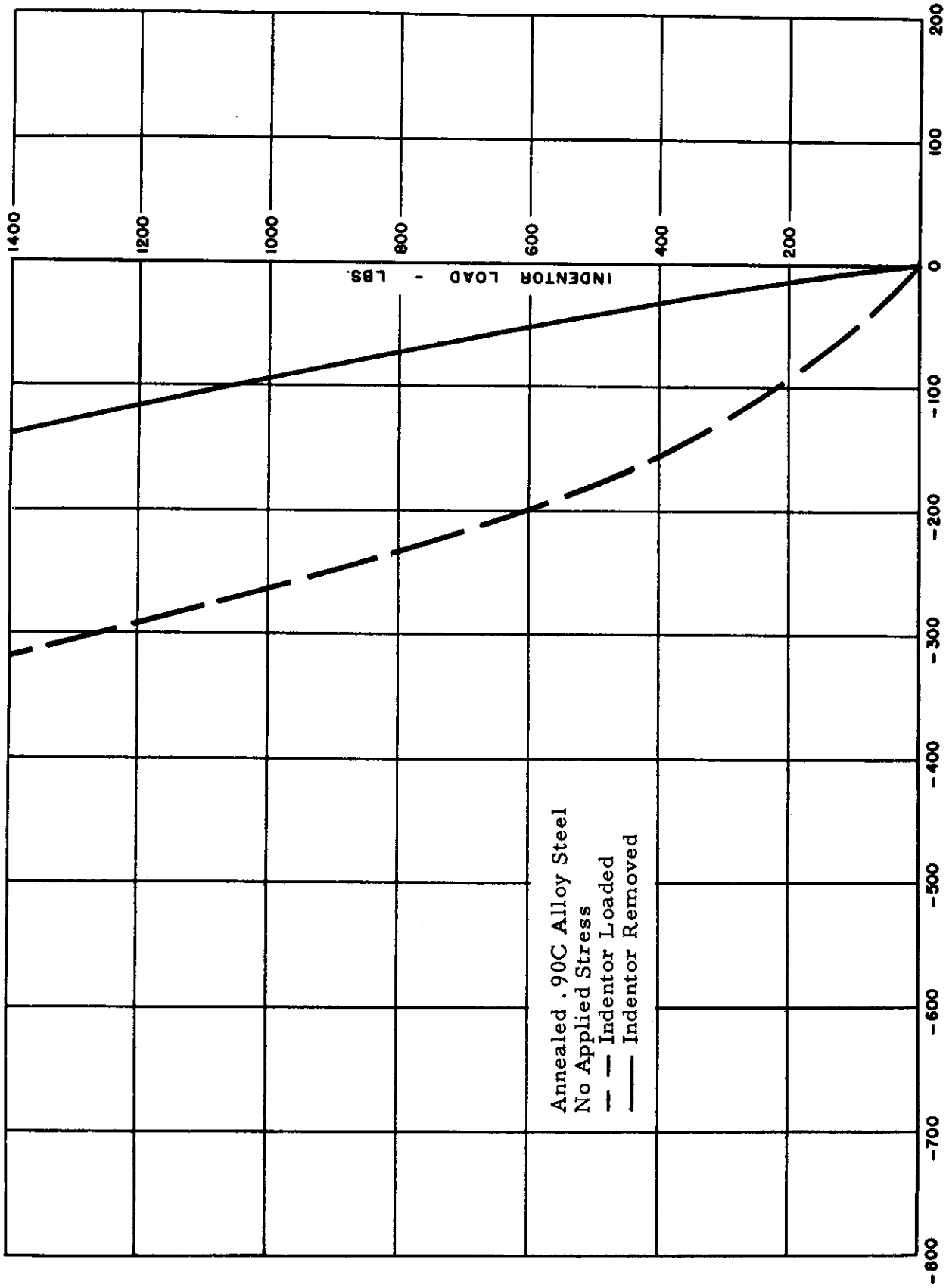

FIG. 15 STRAINS DUE TO INDENTATION

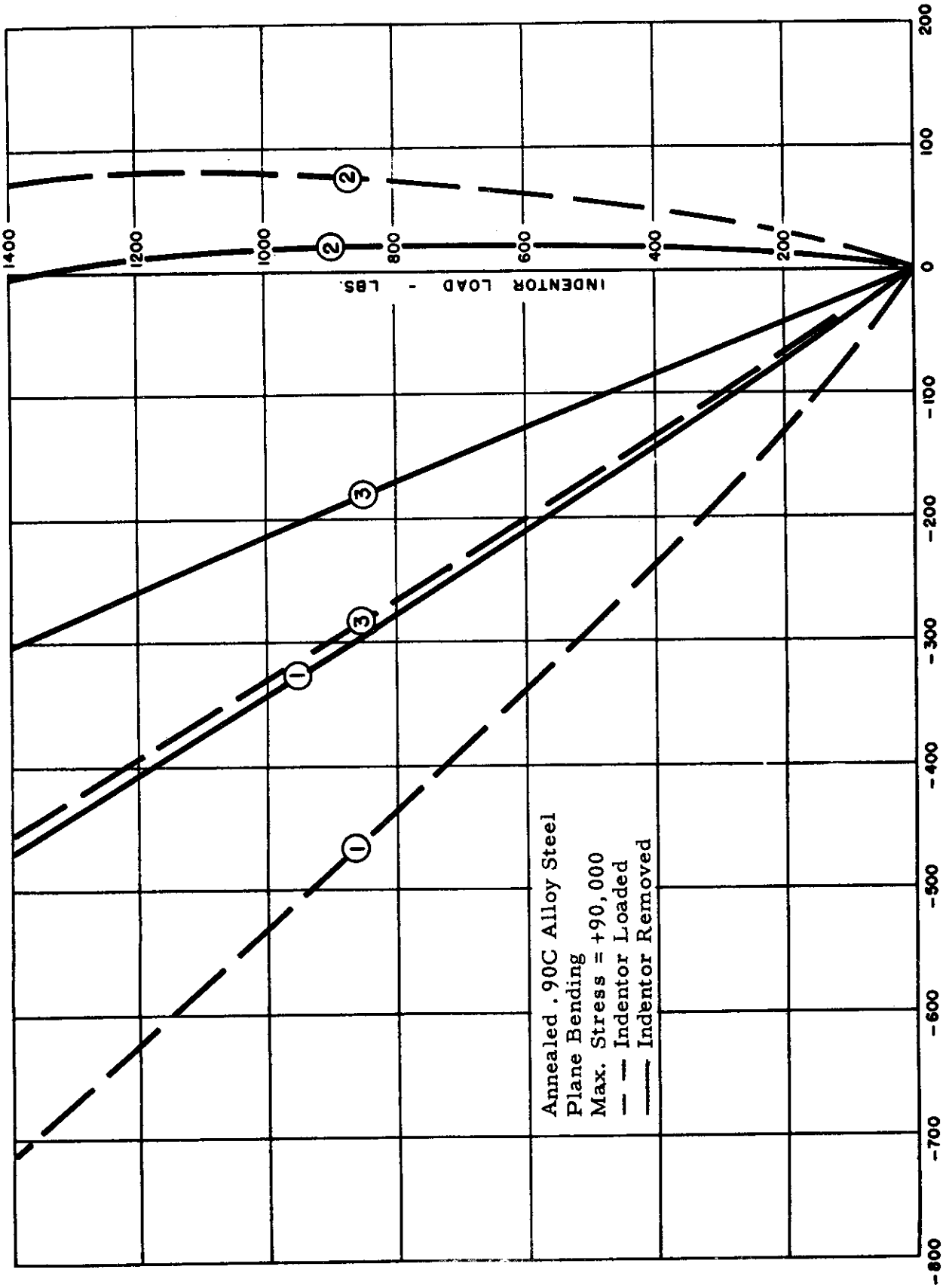

FIG. 16 STRAINS DUE TO INDENTATION

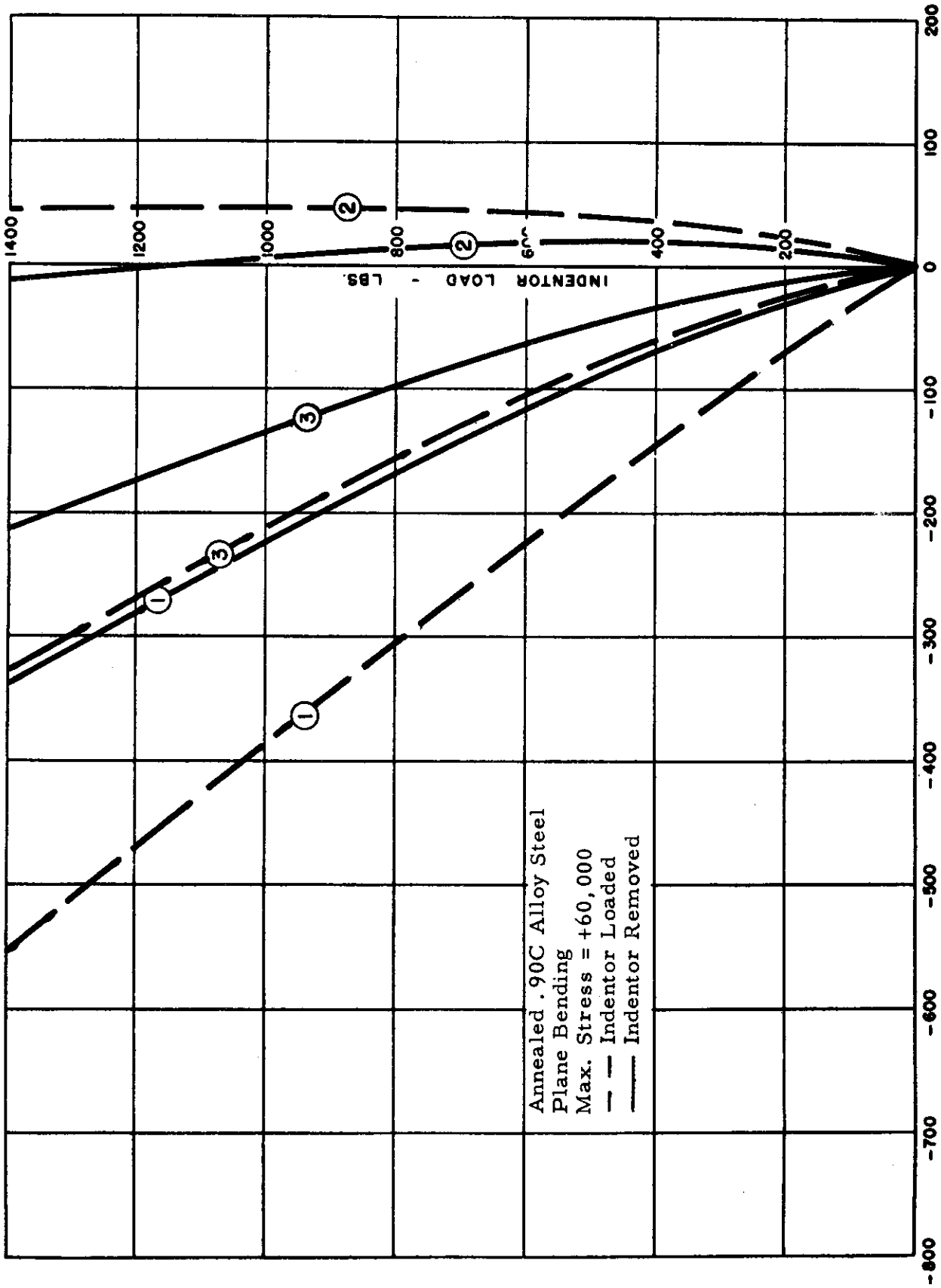

FIG. 17 STRAINS DUE TO INDENTATION

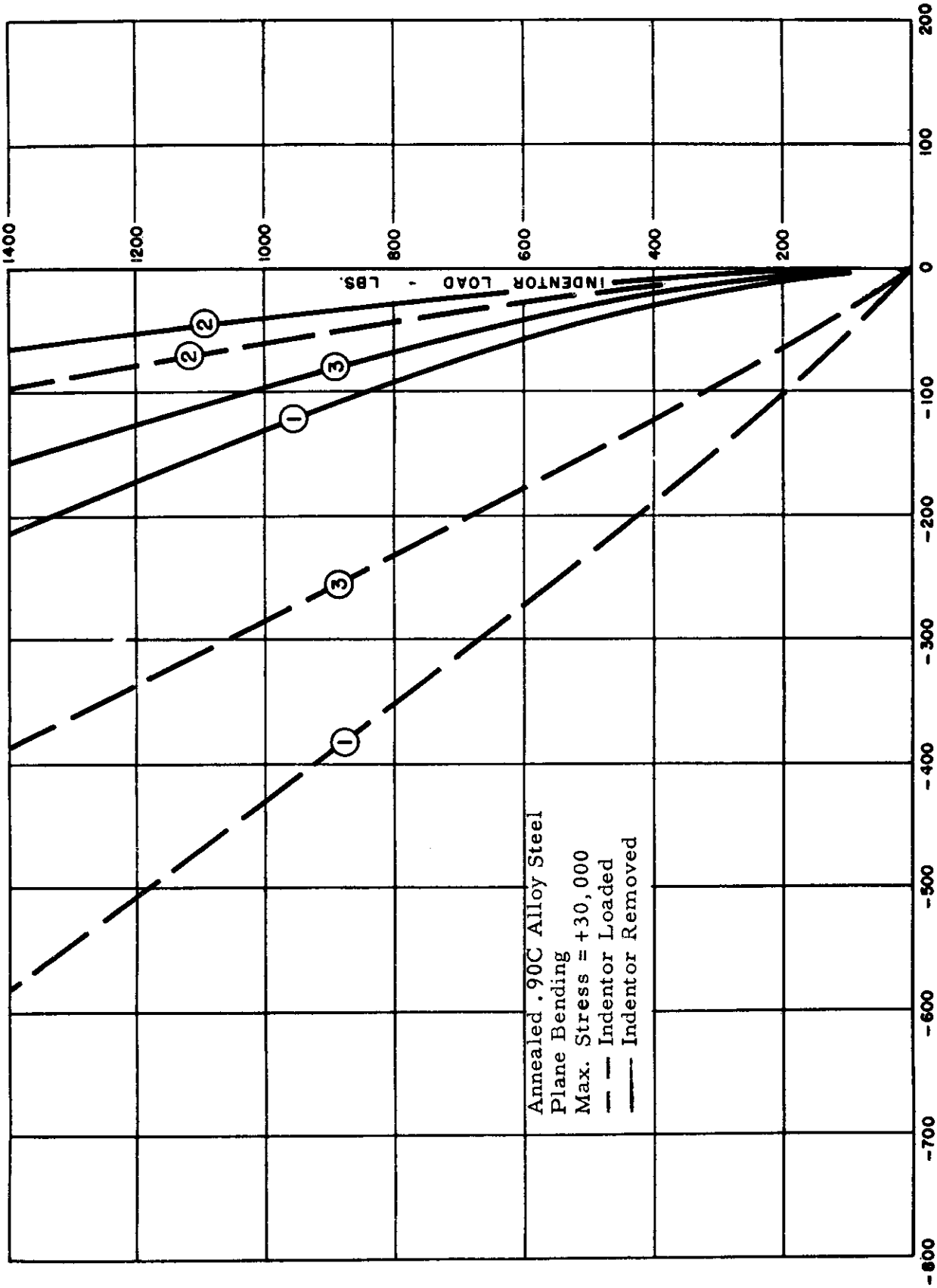

FIG. 18 STRAINS DUE TO INDENTATION

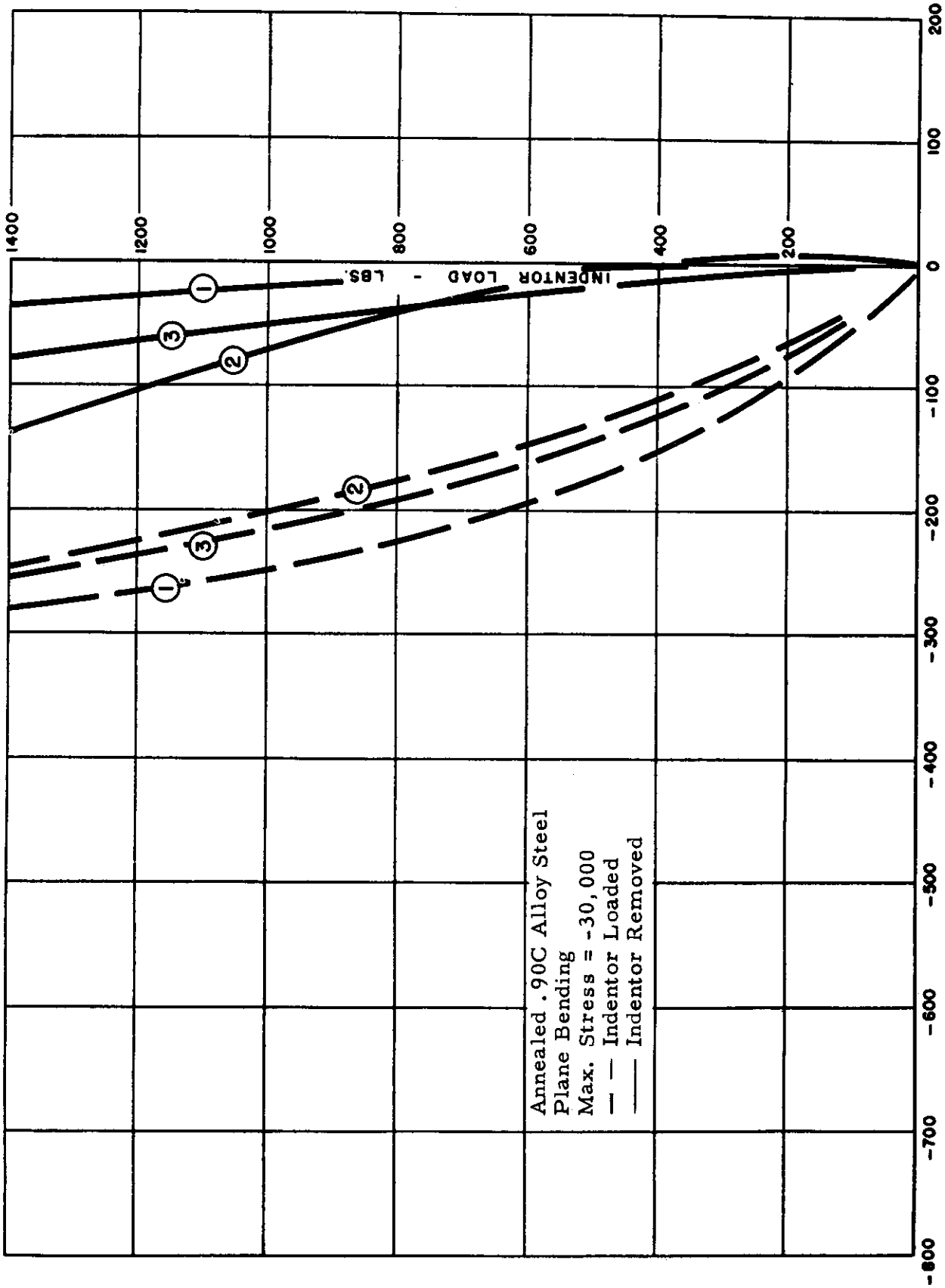

FIG. 19 STRAINS DUE TO INDENTATION

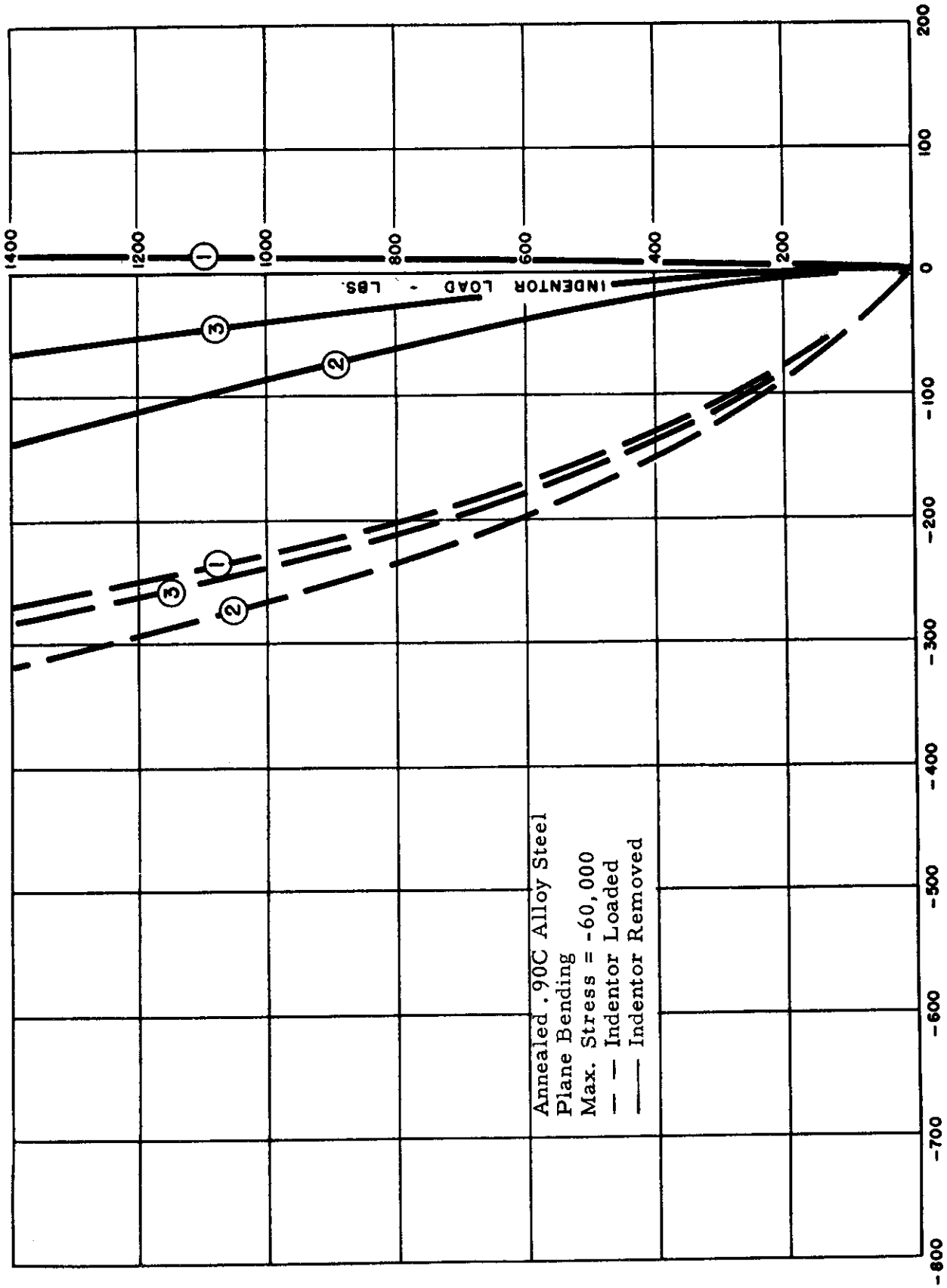

FIG. 20 STRAINS DUE TO INDENTATION

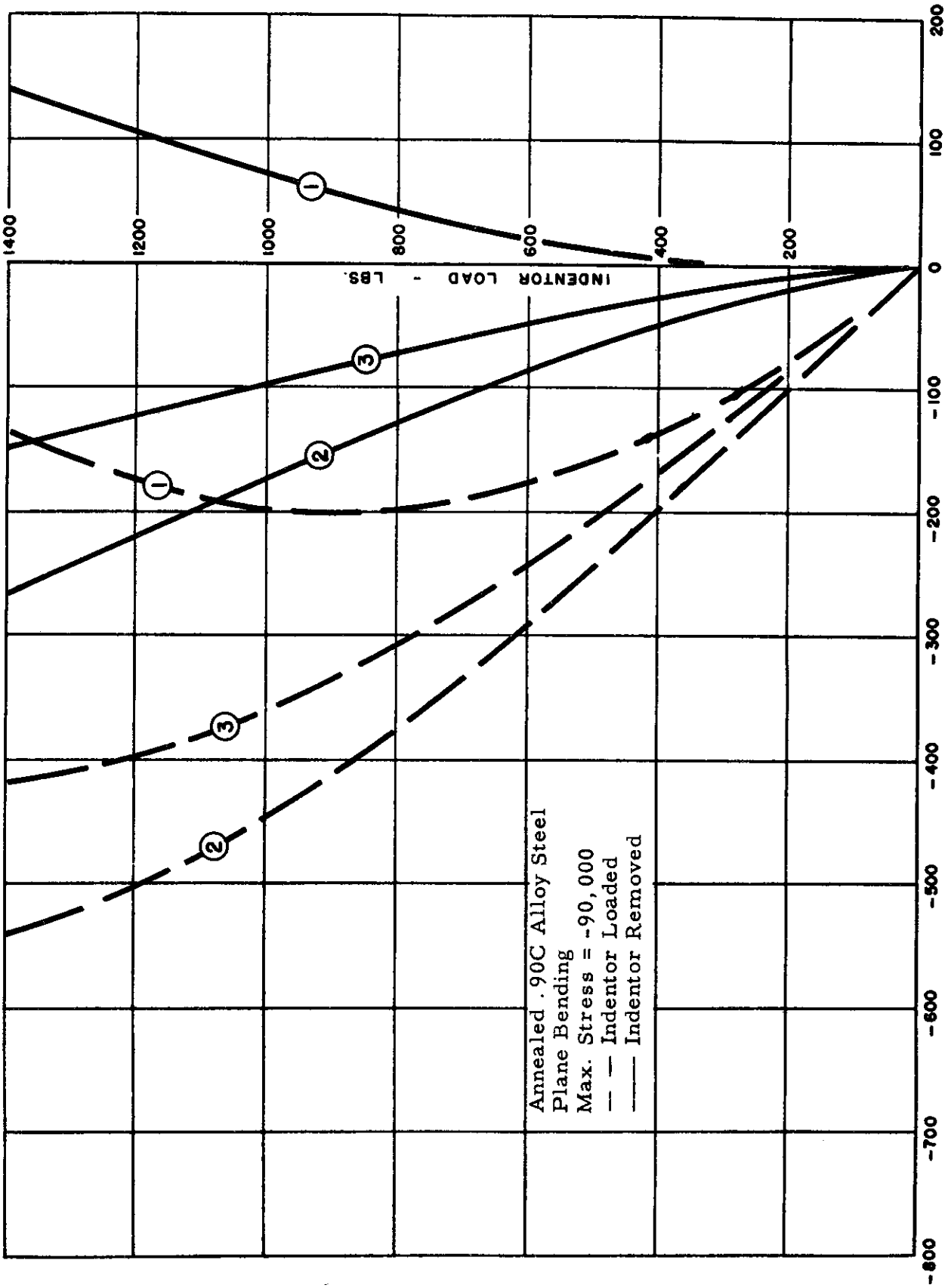

FIG. 21 STRAINS DUE TO INDENTATION

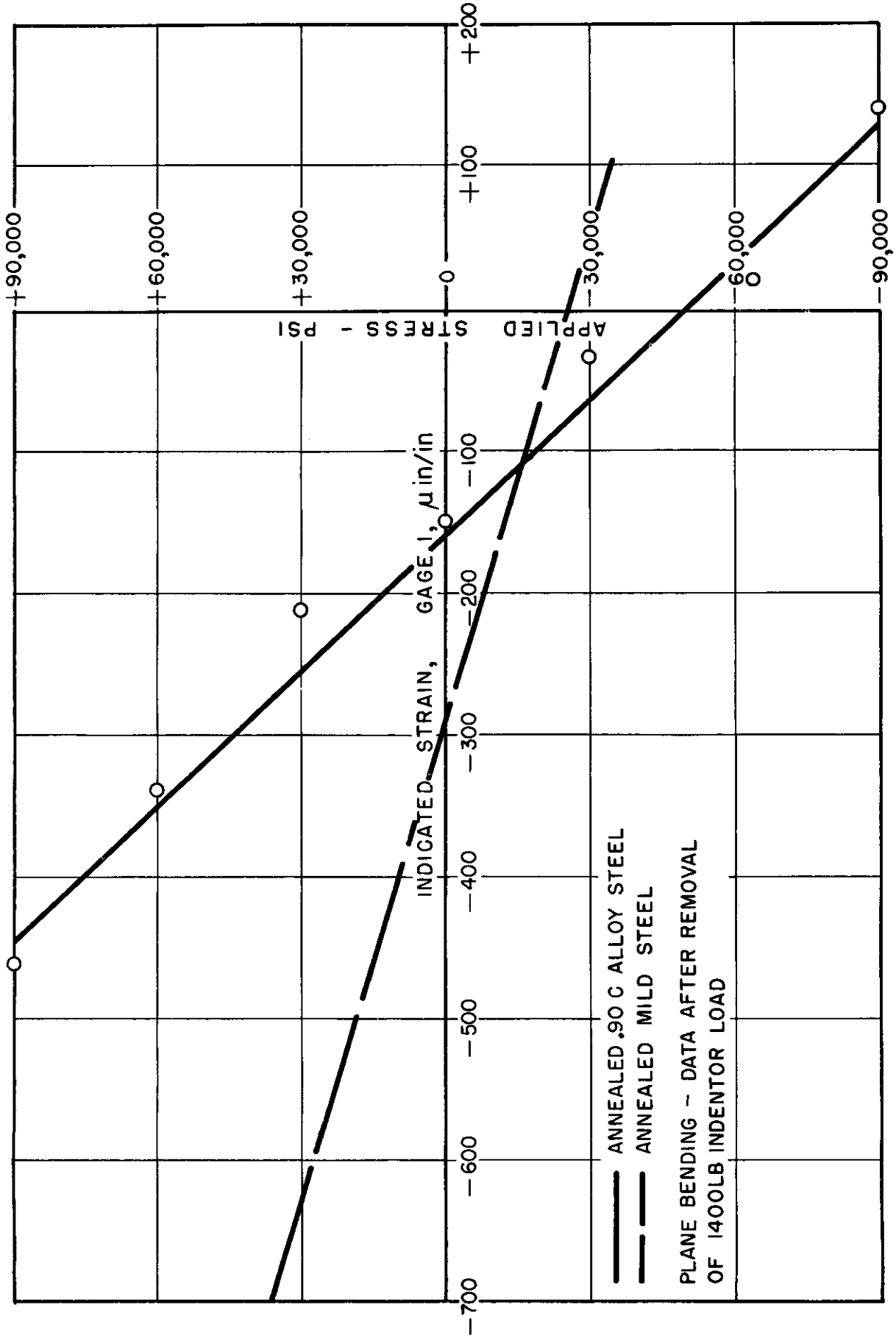

FIG. 22 CORRELATION BETWEEN INDENTATION STRAINS AND RESIDUAL STRESS

These experiments have shown clearly that strains in the surface of a material being indented in this manner are indicative of the residual stress magnitude and direction in that surface. Unknown uniaxial residual surface stresses may therefore be determined in a manner similar to that described below using the data for the .90C alloy steel as an example.

The calibration data, which must be obtained in each case for the particular material being studied, is drawn as a set of curves similar to those shown in Figure 23. The data for these curves is taken from Figures 15 - 21, using the indicated strains after removal of the 1400 lb indentor load.

An indentation test is now made on the specimen under consideration, following the procedures outlined above. The three indicated strain values obtained, separated by known angular spacings, are then fitted to the curve in Figure 23 which best suits them; for example, the three points 1, 2, and 3 which are seen along the +90,000 psi curve. This fitting immediately determines the magnitude of the principal stress. The direction of this stress with respect to either of the three strain gages is measured along the abscissa from the data point to the zero degree ordinate. In the case demonstrated here the direction of this principal stress of +90,000 psi in tension is 34° counterclockwise from Gage 1.

D. Conclusions

These tests have indicated how the heavy indentation method may be used to determine the magnitude and direction of uniaxial residual surface stresses. The technique requires that the surface under examination be indented in a manner similar to the Brinell hardness test. Surface strains in three directions surrounding indentation are recorded during and after the indentation. These strains are related to the residual stresses in a manner which may be determined by properly designed calibration tests on similar material.

It is not suggested that this technique will replace the relaxation methods presently used in the laboratories for the precise determination of stresses in depth. However, where it is required to have some measure of the surface stresses in machine parts without destroying their further usefulness, the indentation test might well suffice. In the case of cyclic loading, where residual stresses are most significant in their effect on service life, it is the surface stress which plays the major role according to present knowledge.

Time did not permit the investigation of the applicability of this method to the determination of biaxial stresses. However, it seems quite in order to assume that similar results can be obtained for the solution of this case.

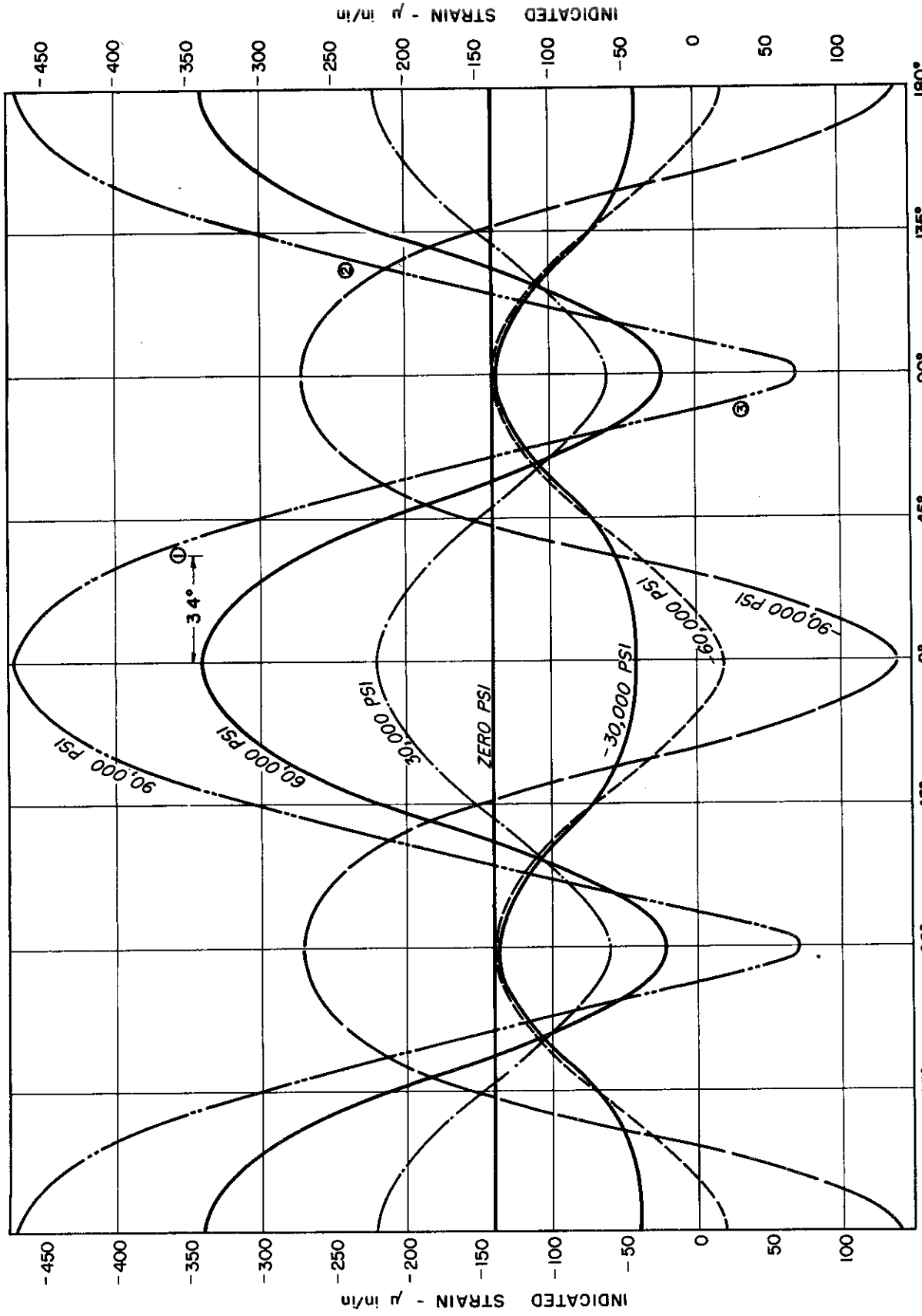

FIG. 23 INDENTATION STRAIN VERSUS ANGULAR POSITION FOR VARIOUS VALUES OF UNIAXIAL STRESS

III. LIGHT INDENTATION

As has been previously stated, the light indentation method depends upon the detection of the indentor load at which the deformation of the surface being indented changes from elastic to plastic. It is proposed that this indentor load will be a function of the residual stresses in the material under test.

One of the early discussions of this concept is by Hoenig (3), his work being reviewed in the first technical report under this contract, WADC TR 54-3. A more recent consideration of this subject based on a somewhat different concept is that by Dervishyan (4) et al. They make use of the Hertz solution for the stress distribution in the case of a sphere on a flat plate wherein the maximum shear stress τ_{max} is as follows:

$$\tau_{max} = .0837 \left[\frac{P_{max}}{R^2 (K_1 + K_2)^2} \right]^{\frac{1}{3}} \tag{1}$$

where P = Indentor load
R = Indentor radius

$$K_1 = \frac{1 - v_1^2}{\pi E_1}$$

$$K_2 = \frac{1 - v_2^2}{\pi E_2}$$

v_1, v_2 = Poisson's ratio of indentor and specimen, respectively

E_1, E_2 = Young's modulus of indentor and specimen, respectively

If there is present in the specimen prior to indentation a uniaxial residual stress, the maximum shear stress due to this residual stress will be:

$$\tau_{max} = \frac{\sigma_r}{2} \tag{2}$$

If superposition holds, the maximum shear stress, when both systems act simultaneously, will be:

$$\tau_{max} = .0837 \left[\frac{P_{max}}{R^2 (K_1 + K_2)^2} \right]^{\frac{1}{3}} \pm \frac{\sigma_r}{2} \tag{3}$$

the sign preceding the $\frac{\sigma_r}{2}$ term being positive for tensile residual stresses and negative for compressive values.

If it is next assumed that the maximum shear stress theory of yielding holds, then plastic deformation will occur when the shear stress τ_{max} equals or exceeds $\frac{\sigma_y}{2}$ where σ_y is the yield strength of the material. Setting (3) equal to $\frac{\sigma_y}{2}$ and rearranging terms leads to the following result:

$$P_y = 213.17R^2 (K_1 + K_2)^2 (\sigma_y \mp \sigma_r)^3 \qquad (4)$$

This very simple equation shows the relationship between the indentor load required for yielding, P_y, and the residual stress, σ_r. For increasing values of tensile residual stress the load P_y becomes proportionately smaller, while for increasing values of compressive residual stress the load P_y becomes proportionately larger.

Further reflection on this problem reveals that for any given surface under test, yielding will occur when the indentor load P reaches the minimum value of P required according to Equation 4 when considering the residual stresses in all directions Θ about the center of the indentation. The applicability of this technique is therefore dependent upon the stress pattern in the surface to be tested in the following manner. If the residual stress is uniaxial tension then P_y may be expected to indicate without error the magnitude of this stress. However, if the residual stress is uniaxial compression then P_y will be indicative of the fact that there is no stress at right angles to the applied stress and will have a single value regardless of the magnitude of the compressive stress. If the stress pattern is biaxial then P_y will be determined by the maximum tensile stress present or the minimum compressive stress if there are no tensile values. Furthermore, the value P_y gives no information concerning the principal stress directions. On the basis of this discussion P_y may be expected to vary, in the case of uniaxial stress, according to the solid line in Figure 24.

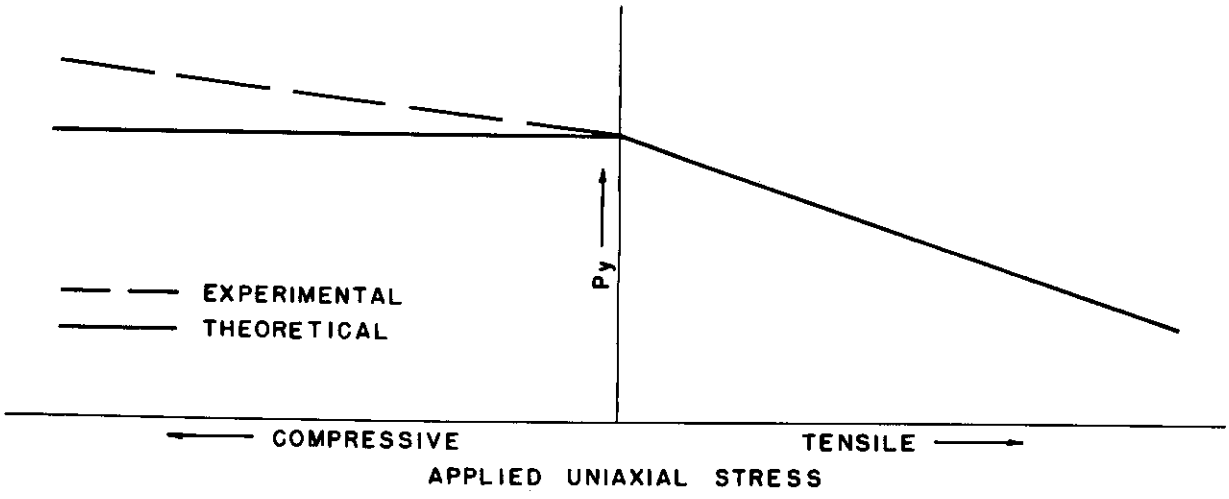

Figure 24. P_y vs. Applied Stress

Tests performed by Dervishyan, op. cit., Sines, Carlson (5), Hausseguy and Martinod (6) show that the variation in P_y is according to the theory where the stresses to be measured are tensile. Where the stresses are compressive these investigators have shown that there is actually a slight increase in P_y, as shown by the broken line in Figure 24. In the light of the investigations into the heavy indentation process discussed in Section II of this report, it appears quite likely that this increase in P_y might well be due to the partial relief of the compressive stresses. It might be argued here that this cannot be true because this technique is carried out in the elastic range and therefore the stress relief found in the heavy indentation test will not occur. However, a closer examination of the methods employed by these investigators to determine the first permanent indentation reveals that their tests were carried into the plastic region and the data extrapolated backwards in order to obtain P_y.

The actual procedure used is to load the indentor in stepwise increments to a major load returning between each increment to a predetermined minor load. The depth of penetration of the indentor at the minor load is recorded each time and a plot similar to Figure 25 is drawn where P_y is taken as the intersection of the data plot (solid line) with the vertical axis. The relief of compressive residual stresses as a result of this indentation may affect the value of P_y in either or both of two ways. With the major load on the indentor, the elastic displacements due to stress relief are in the direction of the indentor and a portion of the load P is required to counterbalance them. The actual load causing the indentor to penetrate the surface is therefore less than that recorded by an amount ΔP, where ΔP is proportional to the compressive stress magnitude. If this effect is taken into account, the data plot will be shifted downwards as shown by the broken line in Figure 25 and a smaller value of P_y will result. Secondly, when the indentor load is reduced to the minor value the effect of these displacements is a shallower indentation than might otherwise be expected. If this effect is also taken into account, the data plot will be shifted to the right by an amount Δa again resulting in a lower value of P_y.

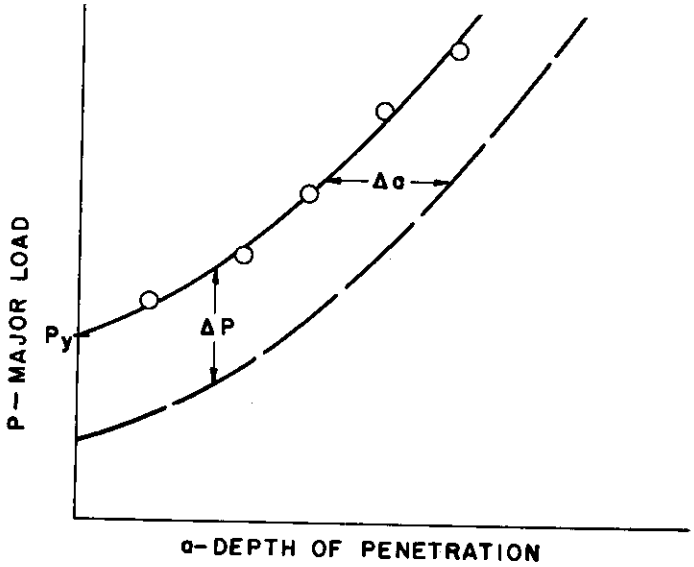

Figure 25. Method for Determining P_y

Although this problem has been stated quite simply and uniquely in mathematical form, the actual performance of the test requires considerable care and thought as to the technique for detecting the indentor load which defines the boundary between the elastic and plastic indentation. Some of the techniques which have been described in the literature are as follows: (1) optical examination of the test surface, Blain (7); (2) change in contact resistance between indentor and surface, Pomey (8) and Brodrick, op. cit.; (3) direct measurement of the indentation depth by noting movement of the indentor along the load axis, Dervishyan, op. cit., and Hausseguy, op. cit.

All of these investigations have indicated considerable difficulty in the actual performance of the test. Hausseguy and Martinod have shown quite clearly that the variation in results for a given test condition decreases with a decrease in surface roughness.

An analysis of the previous work done in this field and outlined briefly above, led to the decision that an exploration of new means for the determination of P_y would yield the most beneficial contribution to the technique. Many possibilities were considered including unique electrical and electronic circuits and optical methods, including the use of the phenomena associated with the interference of light waves. After a careful consideration of the many new techniques which appeared feasible, it was decided to devote the limited time available to a method involving the use of ultrasonic wave propagation in solids.

As the light indentation process is a surface effect, it is reasonable to expect that the transmissibility of ultrasonic surface, or Rayleigh waves, will be altered by it in either or both of two ways. First, the indentation itself will behave as a barrier or reflector much the same as a crack or other defect. Secondly, the transmissibility of the material may be expected to change markedly due to the indentor stresses when the yield point of the material is exceeded. This second phenomenon has been demonstrated in a recent paper by Hikata (9).

In the several experiments which were conducted, a Sperry Reflectoscope Type UR was used employing both a 1.0 and 2.25 mc surface wave transducer. In all instances the single crystal or pulse-echo technique was used wherein a single crystal is used to send out the search pulse and to receive the pulse reflections. A more detailed discussion of the principles of ultrasonic surface waves is given in a paper by Cook and Van Valkenburg (10).

In the first experiment employing this technique, a test bar was subjected to the action of a spherical indentor while being simultaneously scanned by the ultrasonic search unit. A general view of the test setup may be seen in Figure 26. The indentor, a 1 in. steel ball, was mounted in a simple lever system which could be loaded by means of weights at the end of the lever arm. The test specimen was a 1-7/8 in. square 1018 hot-rolled steel bar which had been ground and hand-polished using 600 grit paper.

This test proved negative in that indentations could not be detected until they had reached a size sufficient to make them easily seen using simple optical means. Furthermore, the reflected signal due to the loaded indentor did not vary in going from the smallest possible indentor load to a load many times that required to cause yielding in the test material.

Another test was then designed to indicate the size of indentation or plasticized region which might be necessary for detection in this particular test bar using the surface wave frequencies which were available. Four holes of varying size were drilled in the surface of the bar as shown in Figure 27, and the transducer was mounted to scan the surface. The best results were obtained

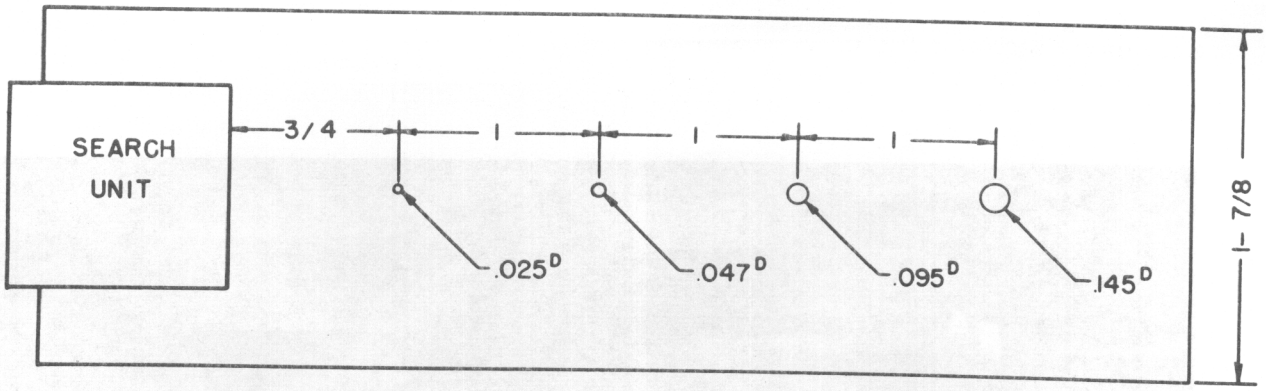

Figure 26. Ultrasonic Test Setup

with the 2.5 mc generator which resulted in a wave velocity of 3.00×10^5 cm/sec and a wave length of .134 cm.

Figure 28 is the reflectogram for this test. The initial signal pulse appears at the extreme left at A, the reflected signals from each of the four drilled holes are B, .025 dia; C, .047 dia; D, .095 dia; and E, .145 dia. The back reflection due to the rear edge of the specimen is at F. The signals at C, D, and E are quite predominant and easily distinguished while that at B is indistinct when compared to the pulses due to the unmarked and polished surface. As the drilled hole at B is of sufficient size to be easily detected by visual examination, it is apparent that the technique, as employed here, is not adequate for this purpose. This investigation was not extended further because of the limitations of time and equipment. Although the results obtained here proved negative, it is quite possible that variations in the technique might well bring it into focus.

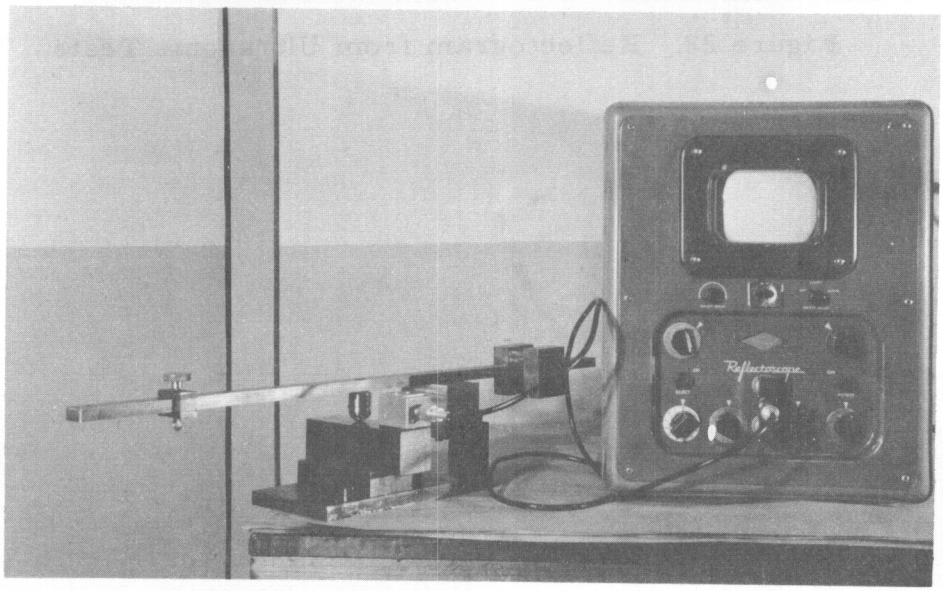

Figure 27. Ultrasonic Test Block

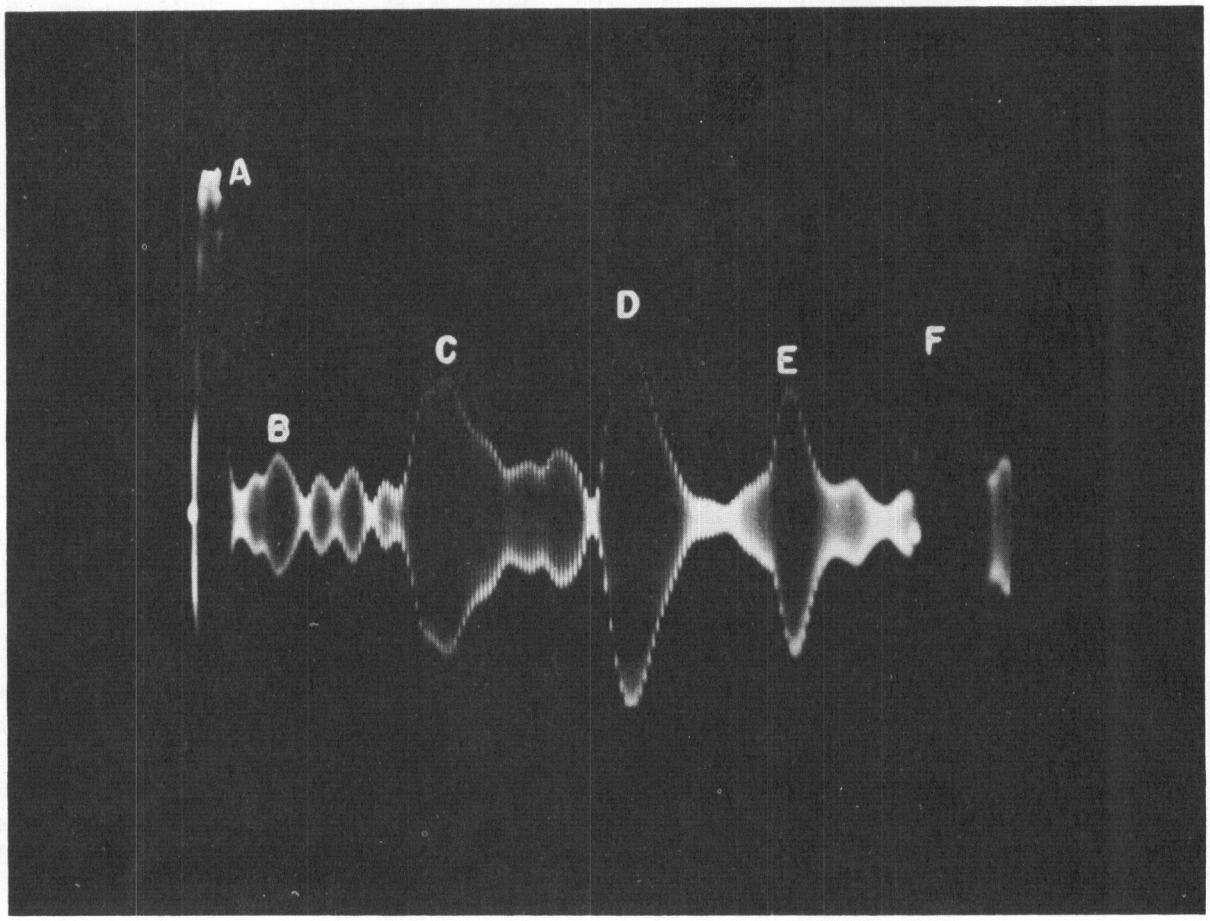

Figure 28. Reflectogram from Ultrasonic Tests

IV. DRILLING OUT

This technique is by no means new in its basic concept having been investigated as early as 1934 by Mather (11). As previously mentioned it makes use of the principles of relaxation through the removal of a cylindrical plug of material from the test piece by drilling or trepanning. The strains on the surface due to this stress relief are related to the residual stress present in the piece. However, the problem of determining the magnitude of stresses below the surface by this method has not been successfully solved to this time and it was this particular aspect of the problem that was studied here. The approach which was chosen was the mathematical analysis of the boundary value problem concerning the dependence of surface strains in the neighborhood of a cylindrical hole upon its depth.

In order to characterize the problem, certain assumptions regarding the stress distribution in the specimen are always necessary since the mere fact that the surface is unloaded is insufficient to determine the residual stresses. The two distributions considered here were those of a uniform uniaxial stress and a biaxially uniform stress both perpendicular to the cylinder axis.

The physically simple configuration of a cylindrical hole of finite depth in a half-space solid leads to an unusual combination of conditions on the stresses. Using a cylindrical coordinate system, the general expressions for the stresses may be written:

$$\sigma_r = \sigma_r\ (r, \Theta, z)$$

$$\sigma_z = \sigma_z\ (r, \Theta, z)$$

On the unloaded boundary, the stresses take the following special values:

when $r > a$, $\sigma_z(r, \Theta, 0) = 0$, where a = radius of hole

when $r < a$, $\sigma_z(r, \Theta, h) = 0$, where h = depth of hole

when $0 < z < h$, $\sigma_r(a, \Theta, z) = 0$

Thus it is seen that σ_z on the unloaded boundary is zero at all values of r and Θ except when r = a.

These boundary conditions must be satisfied regardless of the particular method of attack. The approaches studied here may be roughly divided into the following groups which are by no means mutually exclusive.

A. Application of the Theory of Notch Stresses

The underlying mathematical principles of Neuber's (12) methods are the selection of a curvilinear coordinate system which fits the shape of the notch, and the computation in this system of the stresses near the apex of the notch by means of his form of the three harmonic function method. In practice the method has generally been confined to problems which may be defined in terms of two coordinate variables.

Since a thorough familiarity with the two-dimensional analog of the cylindrical hole problem should provide a valuable insight into the dependence of

surface strains upon hole depth, Neuber's explicit expressions for stress concentration as a function of notch depth were examined critically. In the cases considered, the graphical relations were quite simple and the analytical expressions elementary, if somewhat clumsy. Unfortunately, his results did not seem capable of affording more than a heuristic basis for extension to the case in question since his asymptotic approximations were generally subject to the assumption that the region immediately exterior to the notch was remote. This assumption was perfectly admissible for his purposes, but since this remote region is the location of choice for strain gages, the hypothesis becomes inconsistent with the objective of this investigation.

B. The Biharmonic Schloemilch (13) Series

It is well known (14) that expressions for stresses satisfying the equilibrium conditions may be constructed from the derivatives of a single biharmonic function if the distribution is axially symmetric. The solution of the problem then depends upon the selection of a biharmonic function for which the derived stresses satisfy the boundary conditions.

A Bernoulli separation argument shows immediately that $\nabla^4 B = 0$ is satisfied by any linear combination of functions of the form:

$$\left[a(k) r Z_1(kr) + b(k) z Z_o(kr) + c(k) Z_o(kr)\right] e^{\mp kz} \qquad (1)$$

where k may be real or imaginary and $Z_n(kr)$ represents a solution of Bessel's equation. Of the many series and integral forms obtained by discrete and continuous superposition, the Schloemilch series appeared to best fit the geometry of the problem. It may be recalled that Schloemilch series are of the form:

$$\frac{a_o}{2(n!)} + \sum_{k=1}^{\infty} a_k \left(\frac{2}{kr}\right)^n Z_n(kr) \qquad (2)$$

and that they are capable of representing a null-function without all a_k vanishing. For example:

$$\frac{1}{2} + \sum_{k=1}^{\infty} (-1)^k J_o\left(\frac{k\pi r}{a}\right) = 0 \qquad (3)$$

for $0 < r < a$. Another example is:

$$\frac{r^2}{2} + \frac{2ar}{\pi} \sum_{k=1}^{\infty} \frac{(-1)^k}{k} J_1\left(\frac{k\pi r}{a}\right) \qquad (4)$$

From which a function may be constructed which is biharmonic and vanishing inside $r < a$ for a particular value of $z = z_o$. The result is:

$$\frac{r^2}{2} + \frac{2ar}{\pi} \sum_{k=1}^{\infty} \frac{(-1)^k}{k} J_1\left(\frac{k\pi r}{a}\right) e^{-\frac{k\pi(z - z_o)}{a}} \qquad (5)$$

the convergence of which has been improved for $z > z_o$. Thus, the general procedure for using Schloemilch series as the biharmonic stress function is as follows:

$$B = r \sum_{k=1}^{\infty} a_k Z_1\left(\frac{k\pi r}{a}\right) e^{-\frac{k\pi z}{a}} + \sum_{k=1}^{\infty} (b_k + zc_k)\, Z_o\left(\frac{k\pi r}{a}\right) e^{-\frac{k\pi z}{a}} \qquad (6)$$

is chosen as the biharmonic stress function from which the stresses are computed (14). Finally the a_k, b_k and c_k are determined from the conditions on the stresses at the surface and at infinity.

While this is in principle quite straightforward, it is in practice rather difficult to determine the correct values of the coefficients without a fortuitous selection.

C. Generalization of the Kirsch (15) Formulae

In the Neuber form of the three harmonic function method, the stress field is derived from a stress function:

$$F = A + \overline{R} \cdot \overline{G} \qquad (7)$$

where $\nabla^2 A = 0$, $\nabla^2 \overline{G} = 0$ and $\nabla^4 F = 0$. It has been shown (12) that only three of the four harmonic functions are essential to the solution. If the problem is expressed in cylindrical coordinates:

$$F = A + r(B_1 \cos\Theta + B_2 \sin\Theta) + zC \qquad (8)$$

and it is assumed that $B_1 = (\cos\Theta)B$

$$-B_2 = (\sin\Theta)B$$

and A, B, C are independent of Θ then:

$$F = A + rB \cos 2\Theta + zC$$

$$\text{where } \nabla^2 A = \nabla^2 C = 0 \text{ and } \nabla^2 B = \frac{B}{r^2} \qquad (9)$$

It will be recalled that the cubical dilatation is proportional to $\nabla^2 F$ so that it is of the form:

$$\frac{\partial}{\partial(\ln r)}\left(\frac{B}{r}\right) \cos 2\Theta + \frac{\partial C}{\partial z}$$

which yields a cubical dilatation like that of the Kirsch (15) formulae for the

plate with hole under uniform uniaxial tension in the case:

$$B = \frac{a^2}{r} + b_1 z + b_2 \tag{11}$$

$$C = z + c_1 \ln r + c_2 \tag{12}$$

Since no further conditions have been imposed on F, it appears that a great many cylindrical problems may be solved by a stress function of the form Equation 9. The choice of such a form clarifies the role of Θ dependence but does not reveal the type of r, z dependence in the solution which would most readily satisfy the boundary conditions.

Returning to Equation 9 it is observed that integral solutions may be constructed as follows:

$$F = \int\left\{\left[f_1(k) + f_2(k)z\right] Z_o(kr) + f_3(k)r \cos 2\Theta\, Z_1(kr)\right\} e^{-kz}\, dk \tag{13}$$

which gives the harmonic cubical dilatation in the form:

$$g = \int\left\{\left[g_1(k) + g_2(k)z\right] Z_o(kr)\, e^{-kz}\right\} dk$$

$$+\int\left[g_3(k)Z_o(kr) + g_4(k)r Z_1(kr) + \frac{g_5(k)}{r} Z_1(kr)\right] (\cos 2\Theta)\, e^{-kz}\, dk \tag{14}$$

Since the displacements are given by integrals similar to that for the stress function, integral expressions for the stresses may be obtained by Hooke's law. A direct determination of the unknown portions of the integrands would be excessively time-consuming so that the only way of easily determining them is by a judicious identification with known discontinuous integrals. An examination of the available known Laplace and Hankel transforms did not reveal any discontinuous integrals capable of satisfying all of the boundary conditions.

D. Complex Variable Method

All of the previously discussed methods aim at the construction of functions which satisfy the given boundary conditions on the form of boundary given. Another approach is to transform the given boundary into a simpler one. Generally, this type of transformation can only be carried out by conformal mapping of two-dimensional problems. Thus, the problem of the cylindrical hole has here as its analog that of the semi-rectangular groove.

The simplest image of the semi-rectangularly grooved half-plane is an ungrooved half-plane. The mapping which takes the half-plane, (w), into the given configuration, (z), is given by the Schwarz - Christoffel formula.

$$\left(\frac{dz}{dw}\right)^2 = \frac{1 - k^2w^2}{1 - w^2} \tag{15}$$

or

$$z = \int_0^w \left[\frac{1 - k^2u^2}{1 - u^2}\right]^{\frac{1}{2}} du = E(w,k) \qquad (16)$$

so that z is transformed into w by the inverse of this elliptic integral. This mapping is indicated in Figure 29.

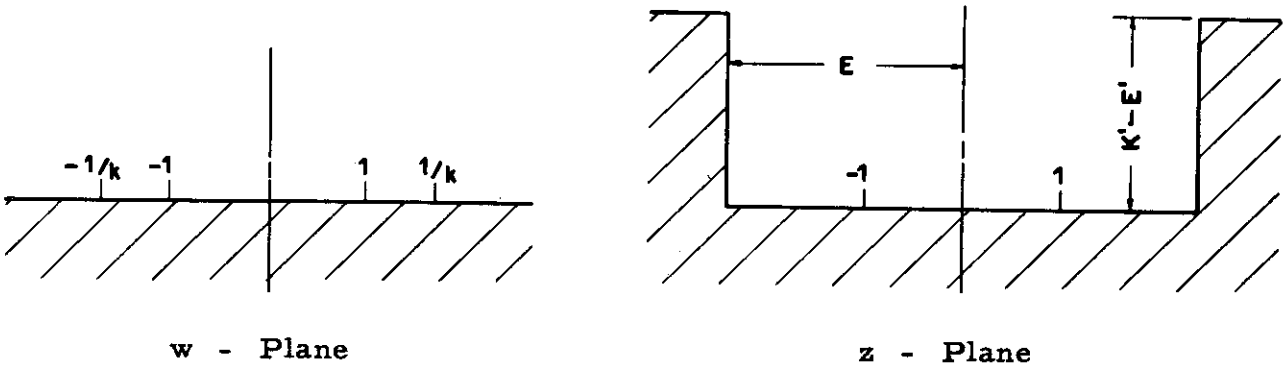

Figure 29. Conformal Mapping of Semi-Rectangular Groove into Half-Plane

Muskhelishvili(16) has given formulae for the stresses in a half-plane in terms of the boundary stresses. These degenerate for the case of an unloaded boundary. However, it appears that a suitable modification of his method could be carried out to obtain the solution for the case of the unloaded groove under uniform tension at infinity.

E. Summary

Although a great many special choices of stress functions possessing various advantages were substituted into the above methods, none of them proved capable of satisfying all of the requirements of the problem. Had more time been available, it is probable that some of the methods would have yielded explicit quantitative information.

For purposes of comparison, it may be of value to consider the line of attack which a purely mathematical investigation of the problem would take. The general question is: What is the relation between the Green's function (dyadic) of a non-convex region and the Green's function (dyadic) of its least convex hull? For the two-dimensional case the starting point is Carleman's Principle of Domain Extension (17). For the three-dimensional problems, very little is known. The case of stress analysis is complicated by the fact that a single Green's function may only be used in special cases and in these it generally satisfies unusual boundary conditions (unlike those of traditional electrostatic problems). The crux of the general problem is the determination of the role of convexity in the characterization of the Green's dyadic.

BIBLIOGRAPHY

1. Bitter, F. On Inhomogeneities in the Magnetization of Ferromagnetic Materials. Physical Review. Volume 38. No. 7. October-December 1931. pp. 1903-1905.

2. Dykstra, Martius, Chalmers, Cavanagh. Internal Microstrains and the Deformation and Failure of Metals. Nondestructive Testing. Volume 12. No. 1.

3. Hoenig, F. Proposal for a New Process for the Detection and Approximate Determination of Self-Stresses. Berg und Heuttenmannisches Jahrbuch. Volume 182. No. 2. 1934. pp. 70-72. (German)

4. Dervishyan, A. O., Janssen, E. and Hurly, W. C. The Stress-Hardness Relation. Office of Ordnance Research, Contract No. DA-04-495-ORD-310. Report 54-76. September 1954.

5. Sines, G. and Carlson, R. Hardness Measurements for Determination of Residual Stresses. Bulletin, American Society for Testing Materials. No. 180. February 1952. pp. 35-37.

6. Hausseguy, L. and Martinod, H. A New Non-Destructive Procedure for the Determination of Superficial Residual Stresses. La Recherche Aeronautique. No. 37. January-February 1954. pp. 43-50. (French)

7. Blain, P. The Effect of Internal Stress on Hardness. Sheet Metal Industries. January 1949. pp. 135-136.

8. Pomey, J., Abel, L. and Goutel, F. Measurement of Residual Stresses on the Surface of Case Hardened and Tempered Steels. Comptes Rendus, Academie des Sciences, Paris. Volume 228. May 1949. pp. 1565-1567. (French)

9. Hikata, A. Ultrasonic Attenuation in Polycrystalline Steel. Bull. Gov. Mech. Lab., Tokyo. No. 1. 1954.

10. Cook and Von Valkenburg. Surface Waves at Ultrasonic Frequencies. Bulletin, American Society for Testing Materials. No. 198. May 1954. pp. 81-84.

11. Mathar, J. Determination of Initial Stresses by Measuring the Deformation Around Drilled Holes. Transactions of American Society of Mechanical Engineers. Volume 56. 1934. pp. 249-254.

12. Neuber, H. Kerbspannungslehre. Julius Springer, Berlin. 1934. (German)

13. Watson, G. N. A Treatise on the Theory of Bessel Functions. Second Edition. Macmillan, New York. 1944. pp. 618-653.

14. Love, A. E. H. A Treatise on the Mathematical Theory of Elasticity. Fourth Revised Edition. Dover, New York. 1944. pp. 274-277

15. Timoshenko, S. and Goodier, J. N. Theory of Elasticity. Second Edition. McGraw-Hill, New York. 1951. pp. 78-84.

BIBLIOGRAPHY (CONTINUED)

16. Muskhelishvili, N. I. Some Basic Problems of the Mathematical Theory of Elasticity. Third Revised Edition. Translation, P. Noordhoff, Groningen. 1953.

17. Nevanlinna, R. Eindeutige Analytische Funktionen. Julius Springer, Berlin. 1936. pp. 63-106. (German)

******